Phil. Trans. R. Soc. Lond. A **328**, 1–33 (1989) [1]
Printed in Great Britain

A STUDY OF THE RAPID DEFORMATION BEHAVIOUR OF A RANGE OF POLYMERS

BY S. M. WALLEY, J. E. FIELD, P. H. POPE AND N. A. SAFFORD
Physics and Chemistry of Solids, Cavendish Laboratory, Madingley Road, Cambridge CB3 0HE, U.K.

(*Communicated by D. Tabor, F.R.S.* – *Received* 8 *January* 1988 – *Revised* 19 *May* 1988)

[Plates 1–8]

CONTENTS

Polymers are increasingly being used in applications where they are rapidly deformed. However, compared with metals, relatively few studies of their mechanical properties at high rates of strain have been published. This paper describes an investigation of the rapid deformation behaviour in compression of a number of widely used polymeric materials. The necessity of properly characterizing polymers is discussed, as the variation of commercial grades bearing the same name is considerable, and furthermore these materials are much more susceptible to change during storage than say metals. The importance of thermal properties to rapid, and hence adiabatic, deformation is pointed out, and tables of such properties are presented. Extensive use was made of high-speed photography (interframe time 7 μs) to study qualitatively the behaviour of solid discs of polymers at strain rates of 2.5×10^{3} s^{-1}. The framing speed was sufficiently fast to capture fracture initiation and subsequent failure of all the polymers studied, including polycarbonate (PC), which fails in an almost explosive manner. The darkening of heat-sensitive film in contact with deforming discs was also investigated. Quantitatively, this technique was used to check the applicability of Avitzur's analysis (Avitzur (*Israel J. Technol.* **2**, 295–304

(1964)) of a deforming annulus to polymers. Agreement was found to be good and hence friction could be measured *during deformation* at high rates of strain for the first time. Studies were also carried out to determine the best lubricant for rapid compressive testing. Petroleum jelly was found to reduce the friction closest to zero. An optically identical system was set up in an Instron mechanical testing machine both to perform friction studies and to explore deviation from incompressible behaviour. Agreement with Avitzur's analysis was found to be poorer, and no lubricant was found to reduce friction below about 3–4 %. PC, with a very high value of frictional stress, showed evidence of a change in volume. Allowances were made for the elastic indentation of the anvils. Higher strain rates were achieved by using an instrumented drop-weight machine and a direct impact Kolsky bar, both developed in this laboratory. Care was taken to eliminate sources of error, including friction and calibration errors. The strain rate sensitivity of the polymers ranged from 5–15 MPa per decade of strain rate. However, most showed some softening as the strain rate was raised from 10^3 to 10^4 s^{-1}, the exceptions being polybutylene teraphthalate (PBT) and polyvinylidene difluoride (PVDF).

1. Introduction

Polymers are increasingly being used in applications where they are liable to be rapidly deformed. Examples of such uses include: aircraft components exposed to particle impact, crash helmets, shock absorbers, bullet-proof windows, and various military applications (Steer 1986). They are also often formed into finished products by using processes that involve high rates of strain. However, compared with metals, relatively few studies on the high-strain-rate properties of polymeric materials have been carried out: Lataillade *et al.* (1980), listed 17 studies in the previous 25 years, whereas a literature survey done by the present authors uncovered over 80 papers on the topic of rapid deformation testing of metals during the same period.

Any study of high-strain-rate properties of plastics must come to terms with the problems of polymer plasticity. There are two main approaches: the first may broadly be called the continuum rheological model where the stress–strain–strain-rate behaviour is modelled by a set of linear differential equations based on various combinations of elastic, viscous, and frictional mechanical elements. Attempts to take account of the nonlinearities of finite deformations by expressing the problem in terms of sums of multiple integrals are often mathematically intractable (Arridge 1975). These mathematical methods have little or no connection with underlying molecular mechanisms. The second approach is the development of theories of yield based on molecular considerations (Ward 1984), and there are several of these in the literature (Bauwens 1982). A very popular theory is that where yield and flow are regarded as activated processes with associated activation energies and volumes (Bauwens-Crowet *et al.* 1974). There is still debate about the exact nature of the molecular processes involved in polymer deformation, but in view of the large values of the activation volumes (several cubic nanometres; Brady & Yeh 1971), some sort of cooperative process on the microscopic scale is envisaged (Fotheringham & Cherry 1978*a*; G'Sell & Jonas 1981; Lefebvre *et al.* 1985). Whatever the nature of these processes, they are in general recoverable, given sufficient time or a high enough temperature. Thus large strain deformation of polymers is not really plastic (which is irrecoverable), and so is usually dubbed 'anelastic'. Recovery can be complete in amorphous polymers (such as polycarbonate), but semi-crystalline polymers usually show a

residue of irrecoverable deformation due to alteration of the microscopic structure (Fotheringham & Cherry 1978*b*; Adams *et al.* 1986).

Lataillade *et al.* (1984) pointed out that the above theories have only been thoroughly checked for strain rates up to 10^{-1} s^{-1}. At strain rates higher than this, the timescale for the flow of heat away from the specimen becomes greater than the duration of the experiment, so that significant temperature rises are to be expected (Chou *et al.* 1973). This will tend to produce strain softening when the rate of deformation is large, whereas at low strain rates increasing strain and strain rate tend to produce strain hardening (Vinh & Khalil 1984).

Most studies on high rate of strain sensitivity have been done in compression. Such experiments, although easier to do than torsion tests, are subject to two major experimental errors, friction and mechanical inertia (Gorham *et al.* 1984), and these are discussed in more detail later. Failure to attend to sources of error such as friction and elastic stresses has led Briscoe & Nosker (1985) to call into question previously published work where an increase in the strain rate sensitivity was reported for strain rates higher than *ca.* 10^3 s^{-1}, both in conventional Hopkinson bars (Chou *et al.* 1973) and in Taylor Impact (Briscoe & Hutchings 1976; Hutchings 1979; Kukureka & Hutchings 1981). Instead they found that the simplest of models proposed to date, the Eyring-type linear increase in flow stress with log (strain rate), fitted the data up to 10^4 s^{-1} for high-density polyethylene (HDPE). Other workers have had success relating the dependence of the yield stress of polyethylene (PE; Truss *et al.* 1984), polyethylene teraphthalate (PET; Foot *et al.* 1987) and polycarbonate (PC; Steer *et al.* 1985) on temperature and strain rate to dynamic loss peaks. They were able to explain changes that they observed in the strain rate and temperature sensitivity by a combination of Eyring type processes.

A major consideration when determining the mechanical properties of polymers is specifying the material that is being examined (Ashby & Jones 1986). It is never adequate simply to give a chemical name, as different grades are manufactured for the various industrial forming processes, such as injection moulding and extrusion. A whole range of chemicals are added to improve processability, to modify the mechanical properties of the finished product, to change the colour, to alter the friction and wear properties, and to slow down chemical degradation (Mascia 1974). Very often this does not matter, so long as the source of the material and its subsequent processing history is known, for mechanical testing is usually performed with a particular end use in mind (Evans 1981; Turner 1983). However, not only do the original mechanical properties of the various commercial grades of the same polymer differ (even from batch to batch (Hillig 1985)), there are also time-dependent changes due to chemical and physical ageing. Chemical ageing is caused by the breaking and reforming of bonds by, for example, ultraviolet radiation, water, oxygen (Mascia 1974). Physical ageing is caused by the slow trend towards thermodynamic equilibrium of the amorphous, glassy component of the polymer (Struik 1978). This can affect bulk mechanical properties such as the flow stress (Adam *et al.* 1975), and the fracture toughness (Hine *et al.* 1986). Dry nylons have been found to be particularly unstable (Wiesbuch & Richter 1986). The environment in which the polymer is to be used also needs to be considered when planning experiments relevant to end use. For even a very ductile polymer such as polyethylene can be rendered brittle when pressurized in contact with certain fluids (Truss *et al.* 1981), and there is evidence that mechanical properties can be modified by hydrostatic pressure alone (Harris *et al.* 1971) and by several gases (Brown 1971; Barham & Arridge 1979). Thus the various properties required

TABLE 1

Primary polymers studied

polymer	commercial type	specific heat temp/K	specific heat value/(J g^{-1} K^{-1})	melting temp/K	sample	heat of fusion/(J g^{-1}) 100% cryst.	formula mass
N6	Akulon M244H (Natural) from AKZO (Holland)	298 313 (T_g) 313 483	1.49 1.58 2.41 2.63[a]	483*	92±1* (dry)	230[a]	113
N66	Maranyl A100 (Natural) from ICI	298 323 (T_g) 323 533	1.45 1.48 2.22 2.65[a]	533*	95* (dry)	300[a] 190[b]	226
PC	Makrolon 2800 from Bayer AG	298 418 (T_g) 418 560 (max. tabulated)	1.20 1.70 1.89 2.21[c]	403*[d] (608 in equilibrium)	*ca.* 1*	132[d]	254
Noryl	731 Grey from GE (U.S.)	298 373 (T_g) 413	1.45* 1.88* 2.02*	413* (decomposes)	*ca.* 0*	—	—
PBT	Valox 325 from GE (U.S.)	298 383 (T_g) 463	1.57* 2.22* 2.27*	496*	52*	not known[e]	204
PVDF	Kynar 730 from Pennwalt	298 (T_g = 233 K)[f]	1.32*	483[e]	not determined because of risk of damage from HF	106[e]	64

TABLE 1 (*cont.*)

Secondary polymers studied

polymer	temp/K	specific heat value/(J g^{-1} K^{-1}) crystal	amorphous	melting temp/K	sample	heat of fusion/(J g^{-1}) 100% cryst.	formula mass
PTFE	298	0.90	1.02	605[g]	39±1*	82[g]	50
	450	1.15	1.27	604*			
	603	1.35[g]	1.39	(T_g = 220 K)[h]			
PMMA	298		1.37	decomposes	—	—	100
(Perspex)	378 (T_g)		1.69				
	378		2.03				
	550 (max. tabulated)		2.44[i]				
polystyrene	298[d]		1.07	513*	*ca.* 0.5	84[k]	118
	373 (T_g)		1.38				
	373		1.64				
	510[j]		1.95				
PE	298[l]	1.55	2.20	fully crystalline:	114±3*	293[l]	14
	390	2.31	2.49	415[l]	(HDPE)		
	413	2.58	2.57		180±10*		
				HDPE: 387*	(MDPE)		
				MDPE: 395*			
				(T_g = 237 K)[m]			
PES	298		1.37*	amorphous	—	—	232
	503 (T_g)		2.11*	(T_g = 483 K)[n]			
PVC (Darvic)	298		0.94	565*	180*	176[e]	62.5
	354 (T_g)		1.11				
	354		1.42				
	380 (max. tabulated)[f]		1.57				

* Note. Our determination; values of specific heat and latent heat quoted from other sources have been converted from their molar values by using the formula masses given.

References: [a] Gaur *et al.* 1983*a*; [b] Starkweather *et al.* 1984; [c] Gaur *et al.* 1983*b*; [d] Cheng & Wunderlich 1986; [e] S. Z. D. Cheng, personnel communication 1987; [f] Gaur *et al.* 1983*c*; [g] Lau *et al.* 1984*a*; [h] Lau *et al.* 1984*b*; [i] Gaur *et al.* 1982; [j] Gaur & Wunderlich 1982; [k] Judovits *et al.* 1986; [l] Gaur & Wunderlich 1981; [m] Gaur & Wunderlich 1980; [n] Bucknall & Partridge 1983.

should be measured sufficiently close in time to each other on samples with the same source and history so that one can be reasonably sure the experiments are performed on the same underlying material.

Even if this is done, the polymer has been specified only in the broadest of terms because commercial secrecy usually prevents the disclosure of the chemicals used as additives. In addition, a complete materials description ought to include the crystallinity, both in quantitative terms (what proportion of the molecules are arranged in crystallites), and also the finer details of how the crystallites are arranged. Only then could subsequent workers know whether they were comparing like with like. However, the characterization of the crystal arrangements in polymers on the microscopic scale by, for example, permanganic etching (Olley *et al.* 1979) has only recently begun and not every polymer has had an etchant developed for it. Even if this has been done, computing a stress–strain curve from a known distribution of crystallites is a difficult problem (Adams *et al.* 1986; Escaig & G'Sell 1982). However, it is likely to be a useful exercise, for if it were possible to predict the properties of plastics from their chemical nature, distribution of molecular weights, arrangement of crystals, and additive content, then polymers could be more rationally designed for their applications. But such studies are only just beginning (Bubeck & Baker 1982; Brown & Ward 1983; Carr *et al.* 1983; Kardos *et al.* 1983; Michler 1986).

Usually only estimates of the fractional crystallinity are available obtained by, for example, differential scanning calorimetry (DSC), as is the case in the present work. DSC cannot distinguish between the many ways the crystallites could be arranged. Thus two samples of the same polymer with the same latent heat of fusion could have different mechanical properties (Wright *et al.* 1988). Also the derivation of a fractional crystallinity from the latent heat assumes that the thermodynamic properties of the amorphous and crystalline fractions are independent and hence simply additive. Careful examination of the literature combined with their own experiments has led Wunderlich and co-workers to conclude that though this structure-independent model is a good approximation in many cases, there are circumstances in which it does not hold (Lau *et al.* 1984*a*). However, it is necessary to measure thermal properties in a study of rapid deformation, not only to try and characterize the materials, but also because high-strain-rate experiments are intrinsically adiabatic (Chou *et al.* 1973). Also inhomogeneous deformation, such as shear bands or cracks, gives rise to very large temperature rises (Fuller *et al.* 1975; Williams & Hodgkinson 1981; Clutton & Williams, 1981; Swallowe *et al.* 1986). These can, however, be quenched at the melting point if the polymer has a high latent heat of fusion (Swallowe & Field 1982; Field *et al.* 1982). Calorimetry is also invaluable in checking the purity of crystalline polymers, for example polypropylene (PP), which is often sold alloyed with polyethylene (PE). This is clearly revealed as two endothermic peaks in the curves of enthalpy against temperature.

2. Materials used

The thermal properties of the polymers used in this study are listed in table 1. The polymers that were most intensively investigated are six in number, namely: nylon 6 (N6), nylon 66 (N66), polycarbonate (PC), Noryl (which is polyphenylene oxide diluted by polystyrene), polybutylene teraphthalate (PBT), and polyvinylidene difluoride (PVDF). These were subjected to all the mechanical tests hereinafter described, and in addition, their sources are

known and the method of specimen manufacture well characterized (injection moulding). All the discs prepared by this method had diameters of 5 mm. A number of other polymers obtained in sheet or rod form from local suppliers were also studied. These were less well-characterized materials, but were of interest for a number of reasons: polytetrafluoroethylene (PTFE) for its low friction, polymethylmethacrylate (PMMA, Perspex), and polystyrene (PS) as examples of brittle polymers; polyethylene (PE), a soft ductile polymer of great economic importance, and used here as a test of the consistency of the high strain rate measurements; acrylonitrile–butadiene–styrene (ABS), a rubber modified polymer; polyethersulphone (PES), a recently developed tough high temperature thermoplastic; and cellulose acetate (CAc), a material available in thin sheets from which small specimens were cut to achieve very high strain rates. In addition, copper was used to verify the form of the corrections applied to the data as a result of the compliance of the apparatus. Copper was used for this purpose as it is a ductile metal with a yield stress not greatly in excess of the hardest polymers examined. It is also not subject to large amounts of viscoelastic recovery as polymers are.

With the exception of the nylons, all these materials were kept in the laboratory exposed to the ambient humidity. The nylons, however, were received from the injection moulder in a dessicator and stored until the moment of the experiment, with the exception of those specimens it was desired to study fully water saturated, as absorbed water is known to have a strong effect on the properties of nylons by altering the mobility of the molecular chains and thus lowering the glass transition temperature, T_g (Deopura *et al.* 1983). Water saturation was achieved by placing nylon specimens in a closed vessel containing water. The percentage increase in mass of two thicknesses of 5 mm diameter discs of nylon 6 and nylon 66 as a function of time is given in table 2.

TABLE 2

material	thickness/mm	time/days	percentage increase in mass
nylon 6	1	8	8
		11	10
		19	10
nylon 6	2	8	5
		13	8
		21	10
nylon 66	1	8	6
		11	7
		19	8
nylon 66	2	8	4
		13	5
		21	6.5

3. THE VISUALIZATION OF RAPID DEFORMATION BY HIGH-SPEED PHOTOGRAPHY

(*a*) *The behaviour of solid polymer discs*

Often in a rapid deformation experiment only the forces applied to the specimen are measured, usually by means of instrumented bars. High-speed photography has been used to measure the strain in deforming metal cylinders quantitatively (Gorham 1980), but in those experiments the photographs were taken in silhouette so that no record of inhomogeneous material behaviour (such as cracking) could be made. There are three main reasons for

wanting to visualize the rapid deformation of polymers: (i) to study the failure behaviour; (ii) to study the temperature rises associated with both bulk flow and inhomogeneous deformation (Swallowe *et al.* 1986); and (iii) to find the best lubricant, i.e. the one that reduces the frictional stress on the surfaces closest to zero.

The apparatus used is shown in figure 1. The polymer discs are deformed between toughened glass anvils in a drop-weight machine that has been modified to create a light path along the axis of the disc (Heavens & Field 1974). The high-speed camera which films the deformation is of the continuous access type. The interframe time was normally set to 7 μs. The experiment is performed by first raising the drop-weight to a height of 1 m and holding it there with an electromagnet. The camera mirror is then spun up, the room being darkened. When the rotation speed equivalent to the desired interframe time is achieved, the camera shutter is opened and the electromagnet turned off. The weight falls guided by three metal rods. Just before striking the specimen, the weight makes contact with a metal wire providing a short circuit trigger to a xenon flash-tube control box. The flash duration is set to last about half a revolution of the mirror, as the image on the film track has an angular speed twice that of the mirror. The camera has no blind spot. Thus so long as the flash is on while the weight is deforming the specimen, the event is captured. The camera has 140 lenses, so nearly 1 ms of information is available. Sometimes the glass anvils broke after about 0.5 ms. When this happened, they acted as a shatter-shutter, preventing overwriting by the decaying flash. However, if the anvils survive, direct comparison of the final and initial states of the specimen is possible, which is of interest particularly in seeing how uniaxial the loading was.

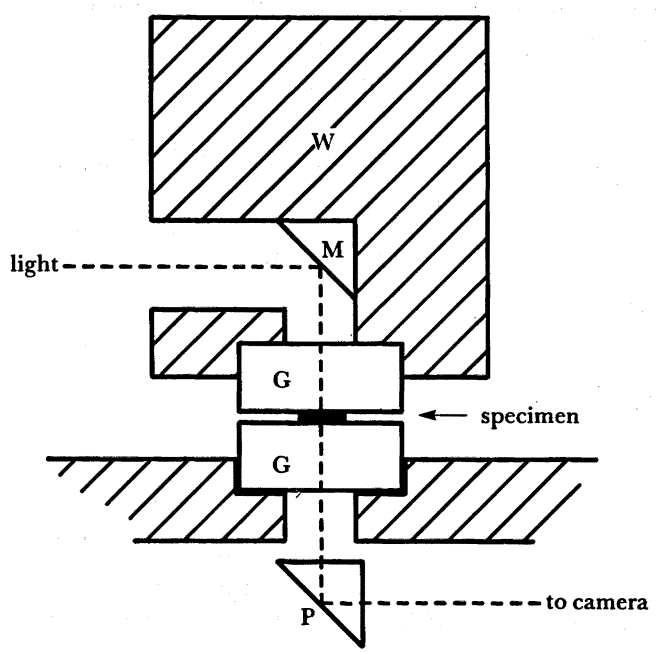

FIGURE 1. Schematic diagram of dropweight apparatus modified for high-speed photography (Heavens & Field 1974). W, weight; M, mirror; G, glass anvils; P, prism.

The conditions for achieving nearly perfect uniaxial loading were found by studying the deformation of annuli (figure 2, plate 1). It was found that if the lower anvil were adjusted in the absence of a specimen so that Newton's rings appeared in the centre of the field of view, then the deformation in the subsequent experiment was axially symmetric. The presence of

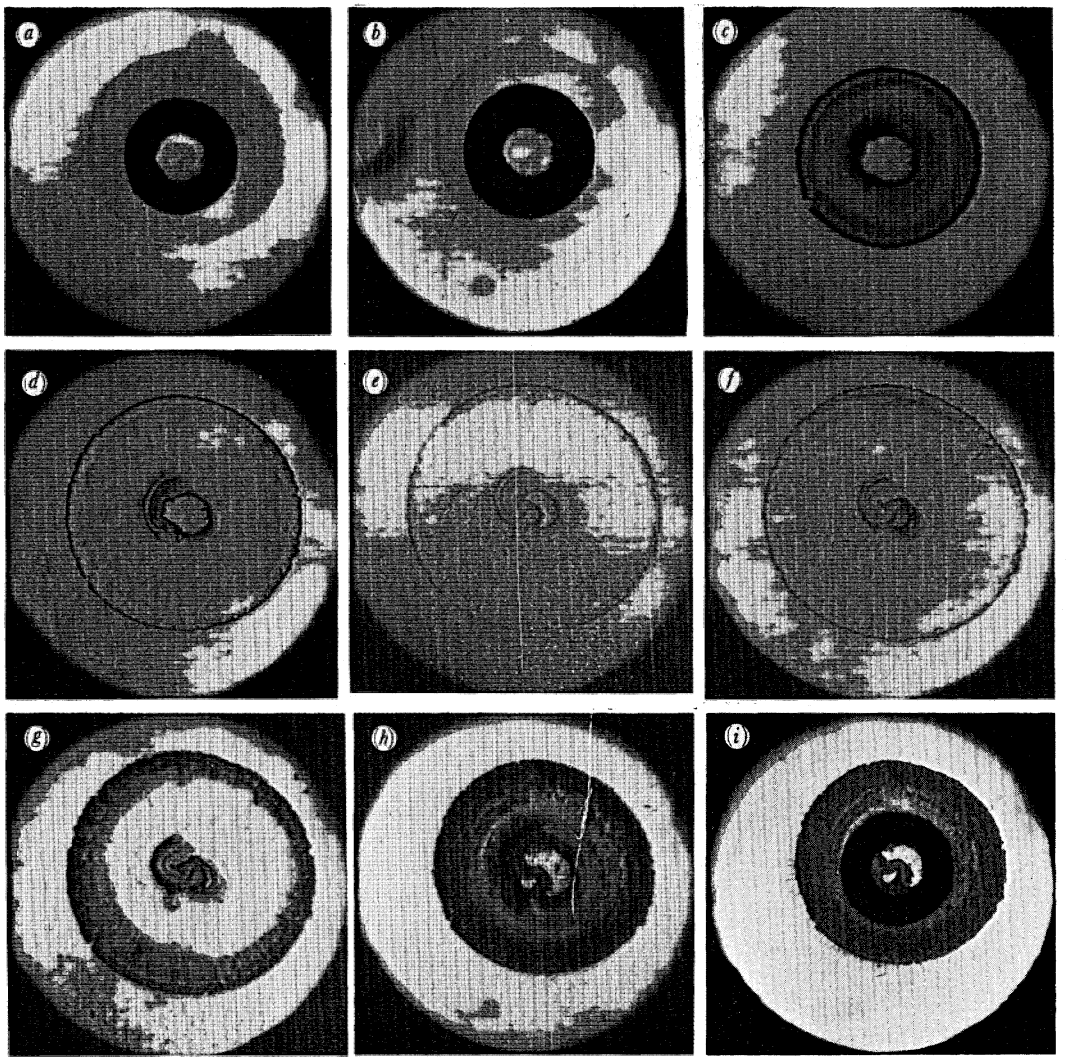

FIGURE 2. High-speed photographic sequence of the unlubricated deformation of a commercial nylon washer (initial dimensions: OD = 6.3 mm, ID = 3.1 mm, thickness = 0.8 mm. Times in microseconds from moment of impact: (*a*) 0; (*b*) 70; (*c*) 140; (*d*) 210; (*e*) 280; (*f*) 420; (*g*) 560; (*h*) 630; (*i*) 700. Note the asymmetric closing of the hole after *ca.* 210 μs and the overwriting in frame (*i*) allowing direct comparison between initial and final states and revealing near perfect uniaxial loading. Unloading is taking place in frames (*g*)–(*i*).

(*Facing p.* 8)

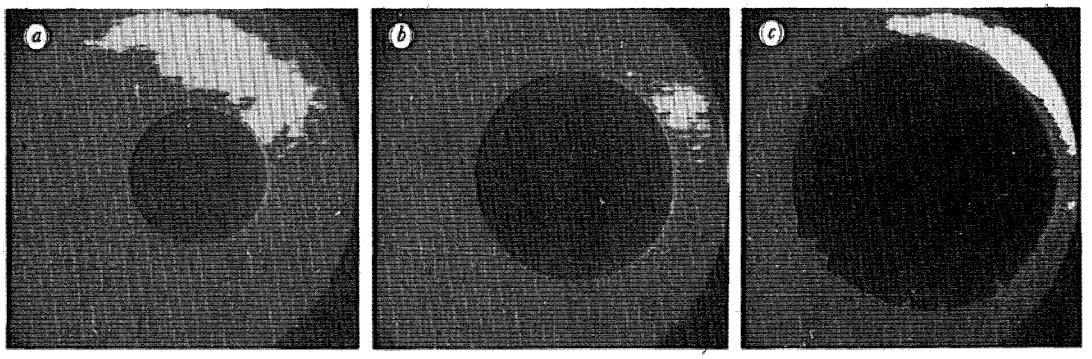

FIGURE 3. High-speed photographic sequence of the deformation and failure of a 1 mm thick and 5 mm diameter Noryl disc (extrusion grade). Times in microseconds from moment of impact (*a*) 0; (*b*) 195; (*c*) 236.

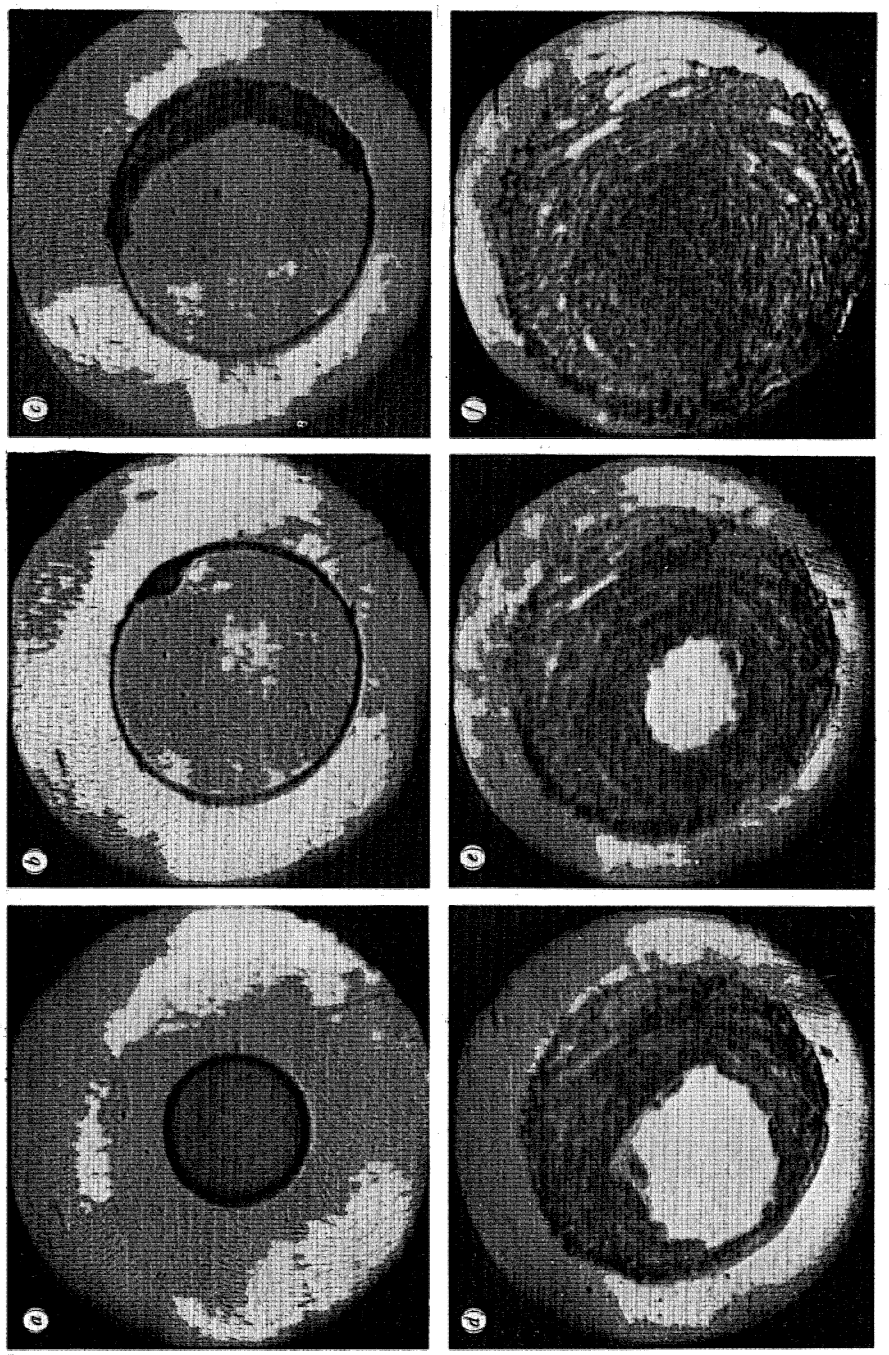

FIGURE 4. High-speed photographic sequence of the deformation and failure of a 1 mm thick and 6.5 mm diameter disc of PES. Times in microseconds from moment of impact: (*a*) 0; (*b*) 263; (*c*) 284; (*d*) 305; (*e*) 312; (*f*) 327.

(*a*)

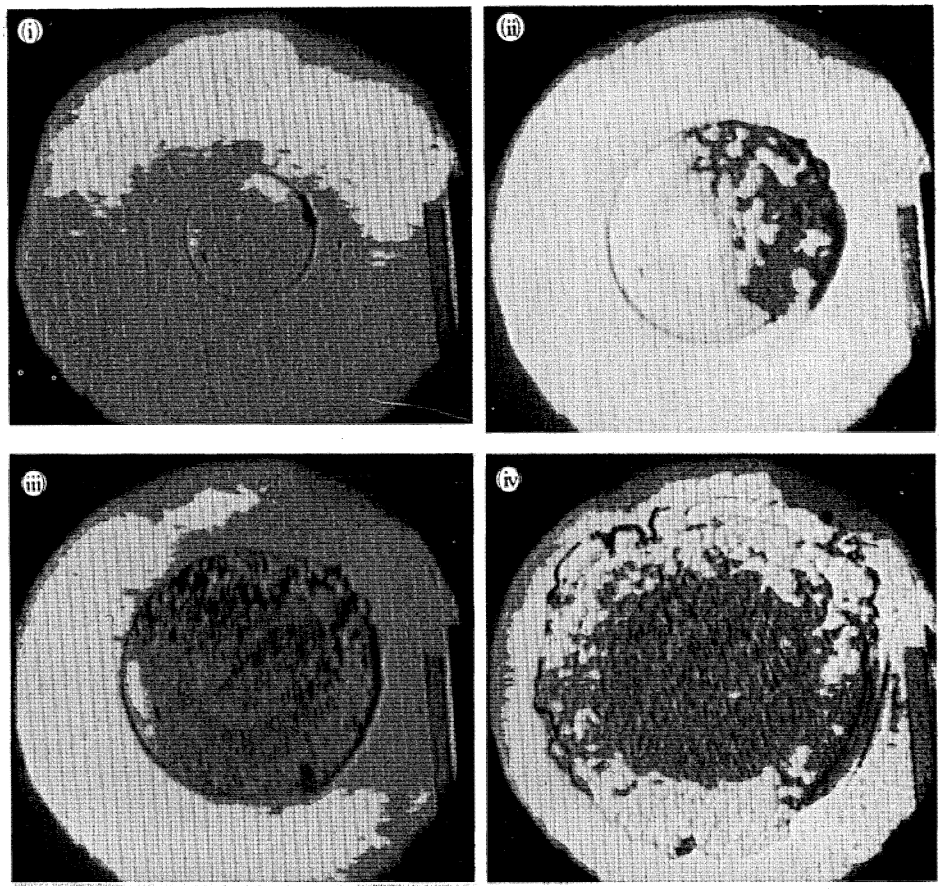

FIGURE 6*a*. High-speed photographic sequence of the deformation of a 1 mm thick and 5 mm diameter disc of PC in contact with heat-sensitive film. Note the development of a ring of discolouration roughly commensurate with the original diameter of the disc, and the buckling of the heat-sensitive film in frame (iv). The darkening of the film during fracture is clearly visible. Times in microseconds from moment of fracture: (i) initial disc; (ii) 7; (iii) 14; (iv) 126. (The original was in colour.)

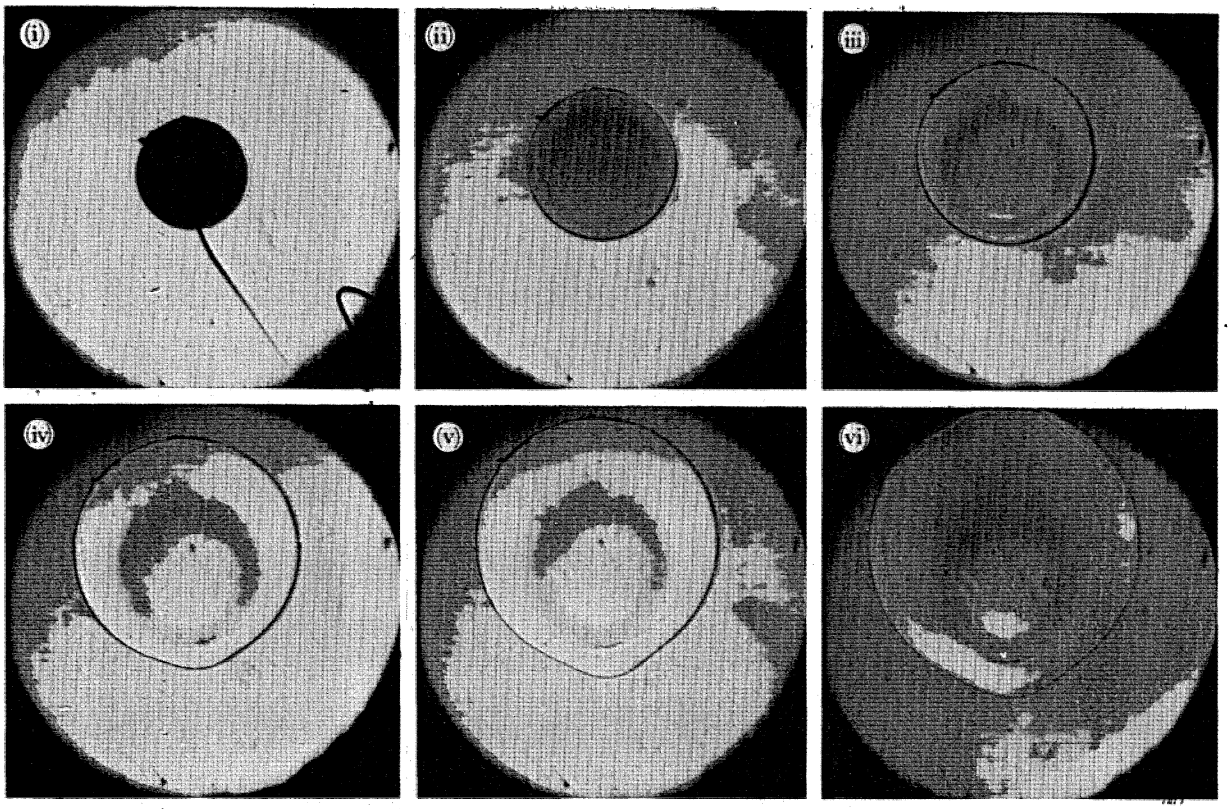

FIGURE 6*b*. Deformation of a 1 mm thick and 5 mm diameter, dry N6 disc in contact with heat-sensitive film. Times in microseconds from moment of impact: (i) 0, (ii) 133; (iii) 175; (iv) 210; (v) 224; (vi) 350. The darkening of the film is clearly visible as a ring that spreads inwards and outwards. The lines in frame (i) were caused by dirt on the camera mirror.

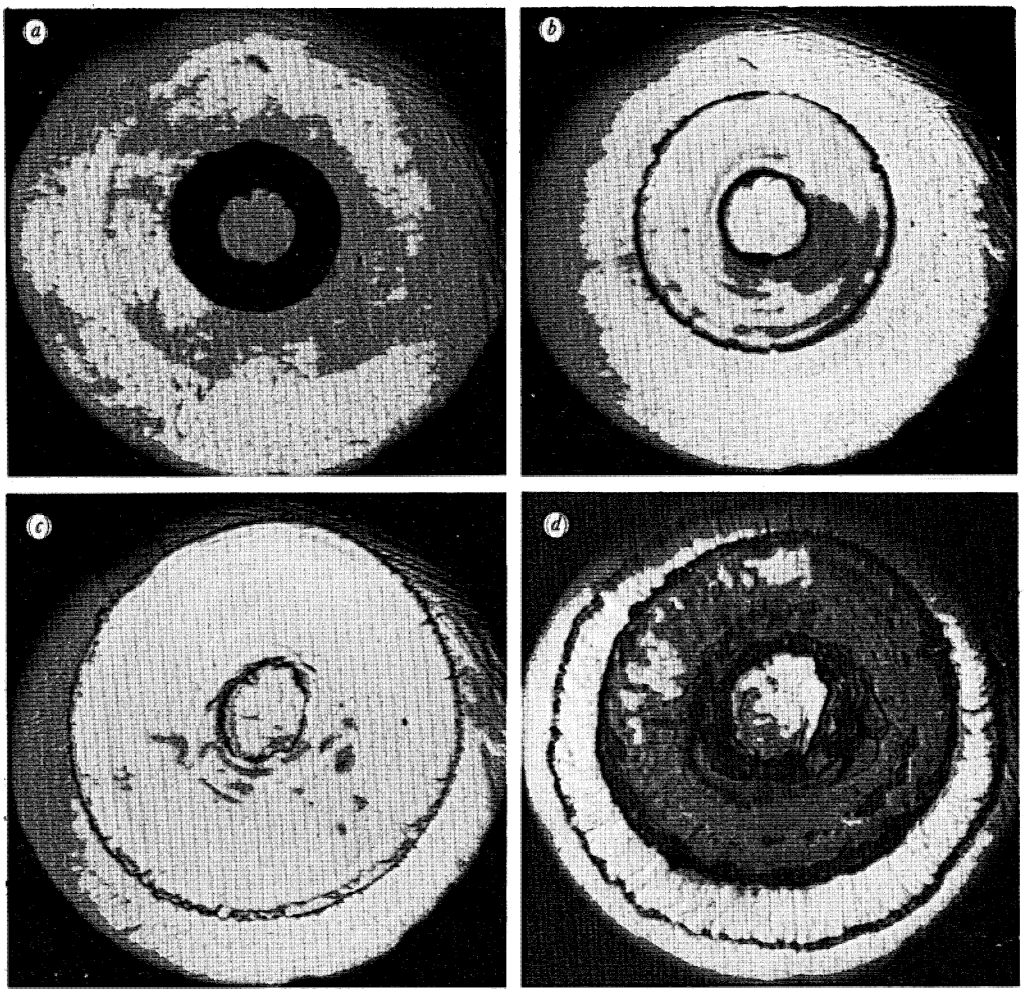

FIGURE 8. High-speed photographic sequence of the deformation of a commercial nylon washer (dimensions given in figure 2) lubricated by gun barrel oil. Times in microseconds from the moment of impact: (*a*) 0; (*b*) 140; (*c*) 210; (*d*) 630. Note in frame (*d*) the substantial relaxation that has occurred on unloading.

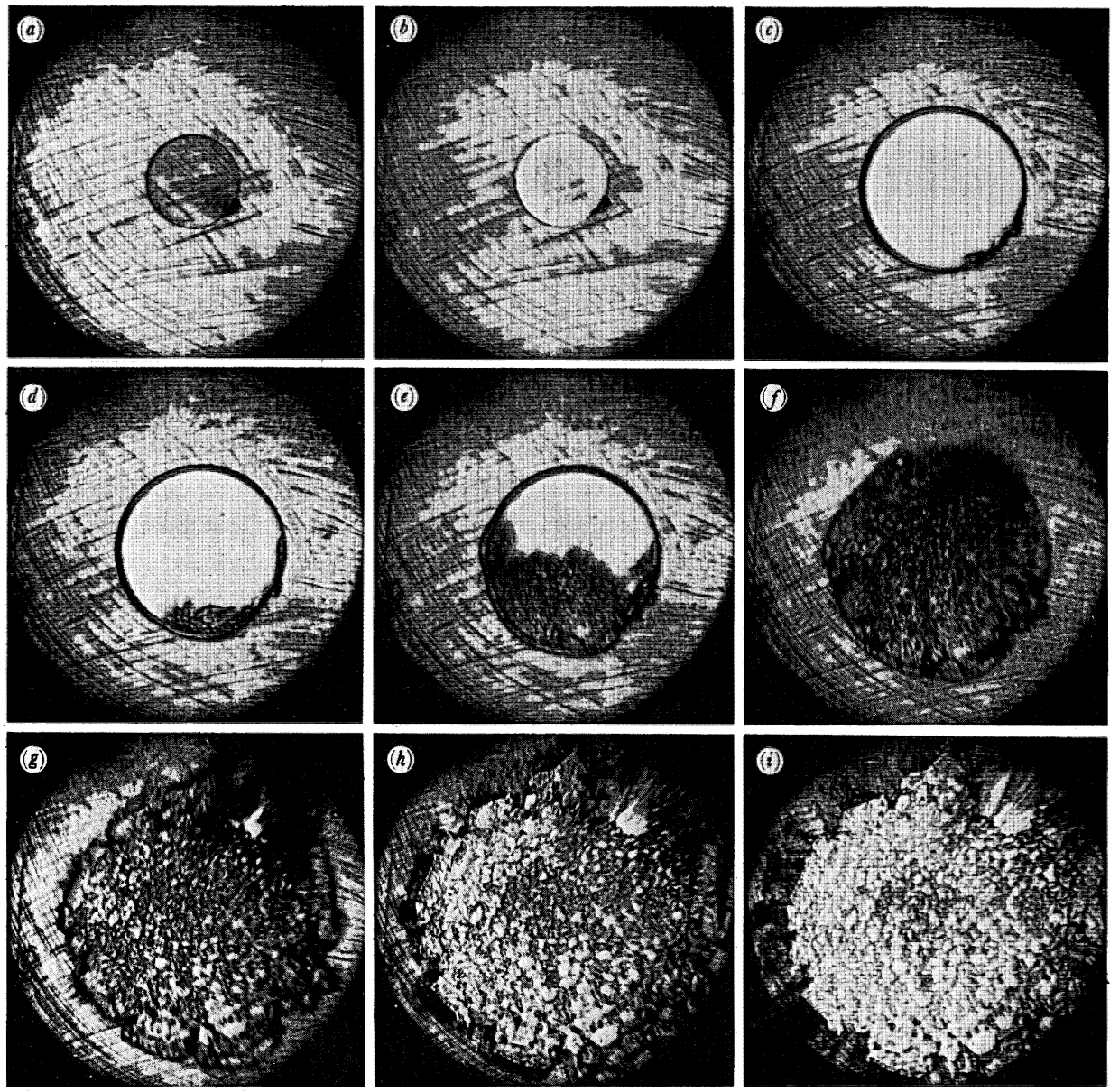

FIGURE 11. High-speed photographic sequence of a 1 mm thick and 5 mm diameter PC disc deforming in the presence of petroleum jelly lubricant. Times in microseconds from the moment of impact: (*a*) 0; (*b*) 14; (*c*) 234; (*d*) 241; (*e*) 248; (*f*) 255; (*g*) 262; (*h*) 269; (*i*) 276.

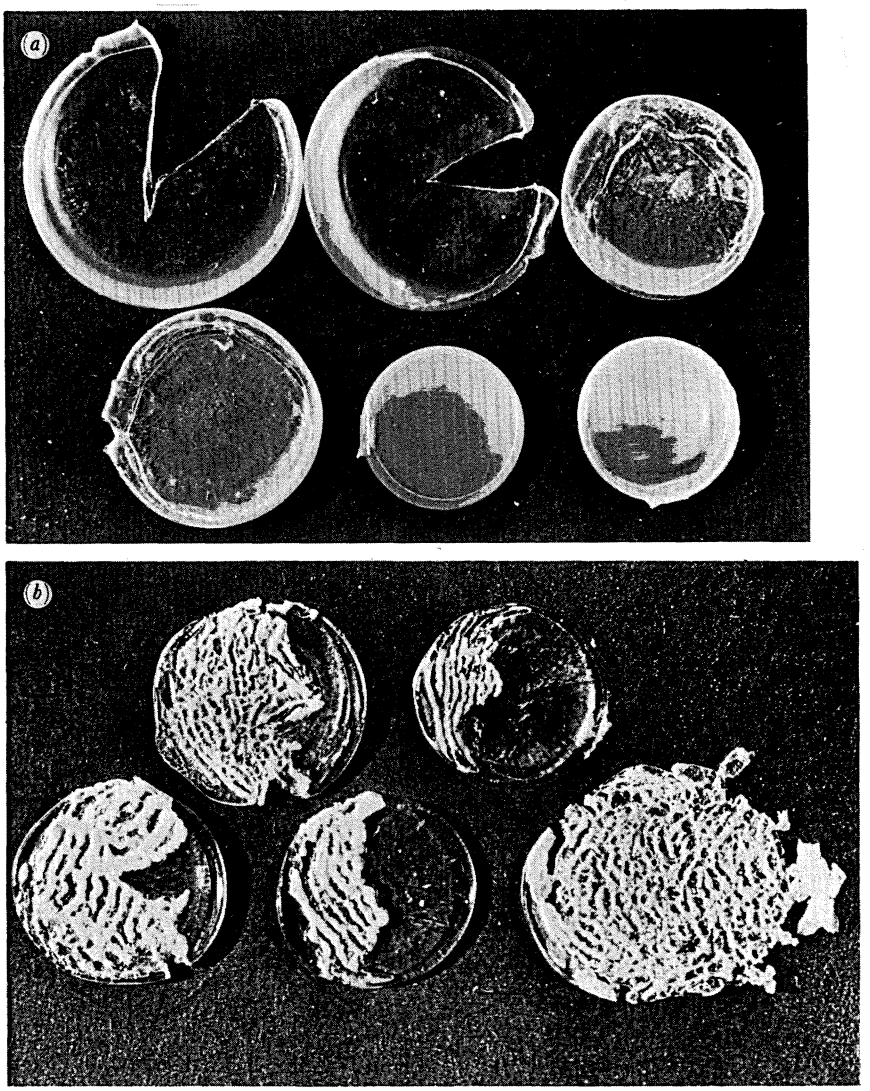

FIGURE 20. Specimens after deformation in the dropweight apparatus: (*a*) 2 mm thick dry N6; (*b*) 1 mm thick PC. Failure was by shear banding.

Newton's rings means that the anvils are not flat. They are, however, very smooth. A Talysurf profilometer on maximum sensitivity (100000×) failed to reveal any surface roughness. Each anvil differed from every other one in its deviation from flatness. Most were convex, but some had regions that were concave. The typical number of fringes visible over a 2 cm diameter area was four, implying about 2 μm of separation at the outer boundary of this area. The small amount of radial traction this produces is more than compensated for by the advantage of being able to align the anvils. Experiments where the anvils were ground flat failed because the anvils always came together to form a wedge, so that the region of no-flow in the specimen was off to one side.

The other departure from the ideal case of a right-circular cylinder deformed between parallel anvils resides in the specimens themselves. These were formed by injection moulding (except for PES) rather than cast individually in a hot press, as it was desired to produce large numbers of reasonably well-characterized specimens quickly and cheaply. Injection-moulded specimens suffer from a number of defects: (i) surface scratches imprinted by the mould; (ii) surface curvature due to shrinkage on cooling; and (iii) internal anisotropy due to rapid flow on injection. The surface defects were investigated with a Talysurf profilometer and optical interferometry. Both techniques showed that the deviation from flatness of the surfaces was *ca.* 10 μm, and every specimen was unique.

The polymers we have examined can be divided into two categories: (i) those that deform homogeneously out to large compressive strains and then contract on unloading; and (ii) those that fail by shear banding and cracking at some strain (Swallowe *et al.* 1986; Walley *et al.* 1985). Since that work was published, several more polymers have been characterized: PBT and PVDF were found to deform homogeneously, whereas Noryl (figure 3, plate 2), PES (figure 4, plate 3), and polyetheretherketone (PEEK) (Walley *et al.* 1987) were found to fail at a strain characteristic of each polymer.

Plots of the strain as a function of time from the moment of impact (see figure 5) allow the strain rate to be determined. The strain values were calculated from the diameter of the specimen as measured from the negatives. Usually every other frame was measured, making

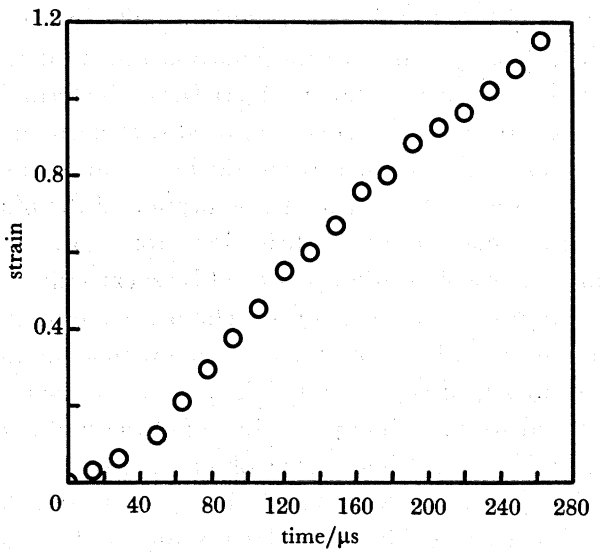

FIGURE 5. Plot of the strain against time for the PES disc shown deforming in figure 4.

the points 14 μs apart. The strain plotted is the logarithmic compressive strain ϵ_c, this being the standard measure in plasticity (Johnson & Mellor 1973). This is defined as

$$\epsilon_c = \ln (h_0/h), \tag{1}$$

where h_0 is the original and h the deformed height. If volume is conserved during deformation and the sides remain vertical, then

$$A_0 h_0 = Ah, \tag{2}$$

where A_0 is the original and A the deformed area of the specimen. If the loading is perfectly uniaxial, the specimen deforms as a circular disc, so that equation (1) becomes

$$\epsilon_c = 2 \ln (d/d_0), \tag{3}$$

where d_0 is the original and d the deformed diameter. In making the plot of figure 5, equation (3) was assumed to hold at all strains. Evidence will be presented later showing it likely that the specimens' volumes were not conserved in these experiments. In which case, the strains plotted will deviate from the true compressive strain but by an unknown amount, as no independent measure of the specimen height was made in these experiments.

The strain rate $\dot{\epsilon}$ may be found by differentiating equation (3) with respect to time, giving

$$\dot{\epsilon} = 2 (\dot{d}/d). \tag{4}$$

From this formula, the strain rates achieved in this apparatus were *ca.* 5×10^3 s^{-1} for 1 mm thick specimens and 2.5×10^3 s^{-1} for 2 mm thick specimens.

(*b*) *The heat-sensitive-film technique for estimating temperature rises*

Since the method of placing a commercial heat sensitive film (3M type 370) in contact with the specimen to estimate temperature rises in polymer deformation was published (Swallowe *et al.* 1986; Walley *et al.* 1985), further studies have been performed on its validity as a technique. The first problem to be addressed is that in its present form it is an invasive technique. The temperature-sensitive mixture is mounted on a polymeric backing sheet, and this will alter the friction at the surface of the specimen. Thus the unavoidable frictional heating at the polymer–film interface is likely to affect the results for bulk temperature rises. Ideally the glass anvils themselves should be coated with the mixture, but although the chemicals it is possible to use have been published in a patent (Wingert 1962) the formulation that is actually used is not public knowledge. Some experiments were tried with petroleum jelly as a lubricant for nylon specimens. The results were inconclusive as the lubricant not only lowers the friction but also slows down the flow of heat. Very little discolouration of the film was produced, and what there was probably occurred where the lubrication broke down.

It is possible that the intense discolouration produced by shear failure or cracking could be caused by chemical effects produced by, for example, chain scission of the polymer molecules. However, experiments conducted with PC specimens coated with an aluminium film deposited in a vacuum also produced intense discolouration. The purpose of the metallic film was to act as a barrier to active chemical species while providing good thermal contact. Both these sets of experiments were conducted without high-speed photography.

Since the work of Swallowe *et al.* (1986), some success has been achieved in filming the darkening process while it is occurring (figure 6, plates 4 and 5). This can only be done with those polymers that start off transparent (such as PC) or go translucent during deformation

(such as nylon). In both cases, the discolouration is first visible as a ring roughly commensurate with the original diameter of the specimen. The ring appears after *ca.* 90 μs in PC, and *ca.* 130 μs in nylon. The ring of discolouration can be seen to become broader with time, spreading both inwards and outwards, the outer boundary lagging behind the specimen expansion. The photographs reproduced here in black and white (figure 6*a*) show less clearly the intense discolouration produced when the PC specimen fractured than do the original colour sequences obtained by Dr R. Sundararajan, where the brown colour was seen to develop within 14 μs of the start of the fracture. Note that the discolouration of the film occurred in the central region of the specimen, and not the periphery, making it unlikely that fracto-luminescence of chemical radicals is responsible for the discolouration.

(*c*) *Dynamic friction measurements*

Measurements of the friction between the anvils and the specimens, both with and without lubricants, were obtained by using annuli of the materials. The analysis used is that of Avitzur (1964, 1968). His analysis was for the uniform deformation of a ring obeying von Mises's yield criterion under uniaxial loading with a frictional stress τ at the interface that is some fraction m of the material's shear yield stress k. He then applied a result from plasticity theory that asserts that the deformation proceeds so as to maximize the dissipation of work, to obtain expressions from which the behaviour of the radius of the hole as a function of the longitudinal compression and the friction parameter m can be computed. Male & Depierre (1970) pointed out that Avitzur also implicitly assumed that the frictional stress is transmitted uniformly throughout the specimen's thickness which will only be close to the truth if the specimen is sufficiently thin. They found that the optimum ratio of outer diameter (OD) : inner diameter (ID) : thickness was 12:6:1, but a ratio of 6:3:1 was adequate under conditions of low friction. In our experiments, the ratio was usually 5:2.5:1, and master curves for the deformation of such annuli for various values of m are given in figure 7. In that and all subsequent figures, the hole strain ϵ_h is defined to be

$$\epsilon_h = \ln (r_i/r_{io}) \tag{5}$$

where r_i is the deformed and r_{io} the initial hole radius. The longitudinal strain was calculated from the area of the annulus using the assumption of volume conservation (equations (1) and (2)).

The annuli were generally made from discs by using a flat-ended punch to form the hole in the centre, although some experiments were also performed with commercial nylon washers and with copper (where the hole was made by spark machining). High-speed photography was necessary to measure the dynamic friction as the annuli sometimes closed up completely (figure 2), or failed by shear (e.g. PC), or recovered substantially on unloading (figure 2 and figure 8, plate 6). If any of these three types of behaviour occurred, measurements on recovered specimens could not yield a value for the dynamic friction, nor determine whether the deformation proceeded according to Avitzur's analysis. In several cases, it was difficult to fit an Avitzur curve to the data, either because the friction changed during deformation (usually at a longitudinal strain of *ca.* 0.4) or because the specimens deformed asymmetrically. The best agreement with theory was found for dry nylon 66, PC, and copper (figure 9); the last named material followed the analysis out to natural strains greater than one.

The lubricant that produces the most uniform deformation in a compression test is one that squeezes out in such a manner that the outwardly directed traction it exerts because of viscous

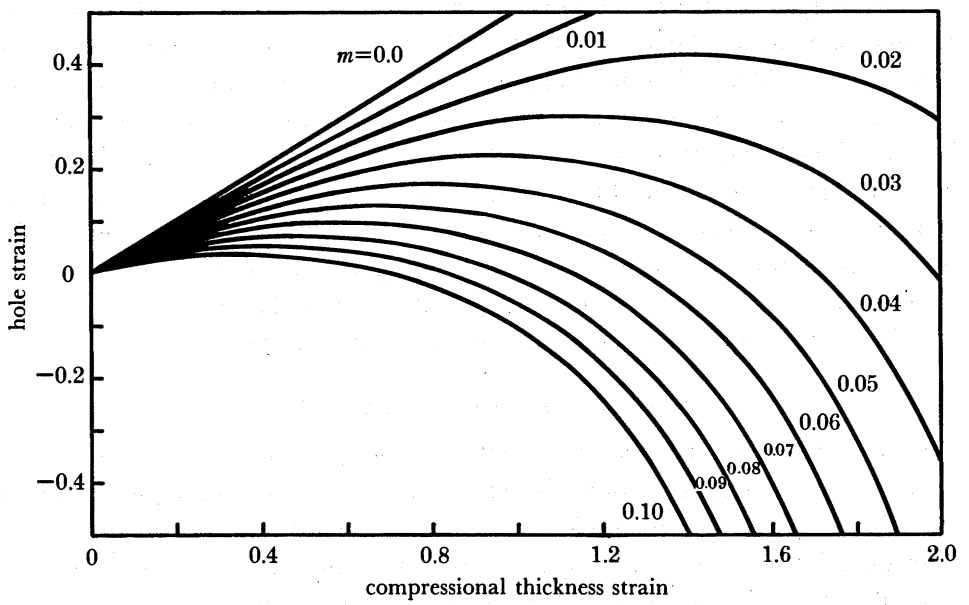

FIGURE 7. Plots of the hole strain against longitudinal compressive strain calculated according to Avitzur's analysis for annuli whose initial dimensions are OD = 5 mm, ID = 2.5 mm, thickness = 1 mm, for various friction parameters.

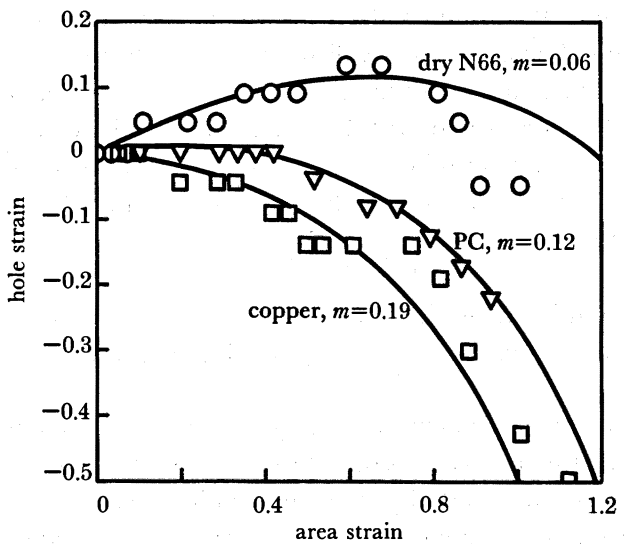

FIGURE 9. Avitzur plots for annuli of three materials deforming in the dropweight apparatus of figure 1. Avitzur curves fit the experimental data well, although dry N66 deviates after a strain of *ca.* 0.8. Both the N66 and PC annuli had dimensions OD = 5.2 mm, ID = 2.2 mm, thickness = 1 mm. The copper annulus had dimensions OD = 5.0 mm, ID = 2.4 mm, thickness = 1.1 mm. Symbols: ○, dry N66; ▽, PC; □, Copper.

drag exactly balances the inwardly directed traction due to shearing of the lubricant between the specimen surface and the anvils (Taylor 1938). This is easier to state than to achieve, especially in impact as the properties of lubricants are radically changed compared to their normal use say in rolling systems (Booth & Hirst 1970*a*, *b*; Hirst & Lewis 1973). Three lubricants were investigated: a silicone grease, a thin oil used to grease gun barrels, and a low-molecular mass petroleum jelly. They were evaluated with commercial nylon washers, and

plots of the deformation obtained are presented in figure 10 when the unlubricated case for comparison. It can be seen that the best of the three is the petroleum jelly, confirming the findings of Briscoe & Nosker (1984) for polymers tested in a Hopkinson bar. Table 3 presents the values of m determined for some of the polymers and copper with and without lubricants.

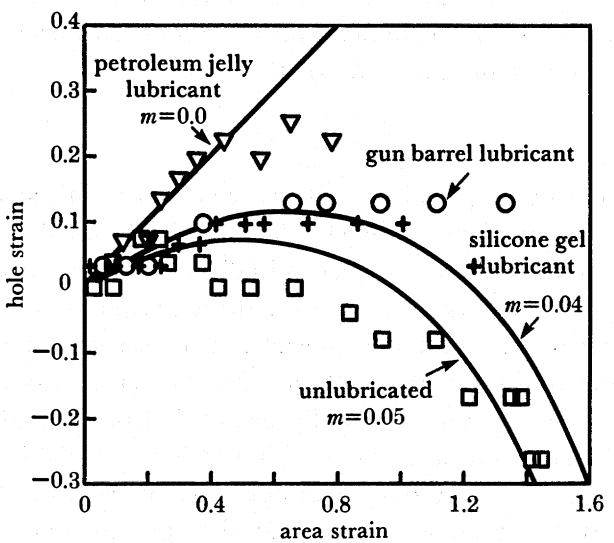

FIGURE 10. Avitzur plots for nylon washers (dimensions given in figure 2) deforming in the presence of three different lubricants, and also unlubricated. Petroleum jelly can be clearly seen to give the best lubrication, though failing at a strain of *ca.* 0.4. Symbols: ▽, lubricated by petroleum jelly; ○, lubricated by gun barrel lubricant; +, lubricated by silicone grease; □, unlubricated.

TABLE 3. VALUES OF AVITZUR'S FRICTION PARAMETER, m, FOR VARIOUS MATERIALS DEFORMED IN A DROP-WEIGHT MACHINE BETWEEN GLASS ANVILS

material	m	notes
dry N6	0.08 ± 0.01	
wet N6	0.11 ± 0.01	
dry N66	0.06 ± 0.01 0.07 ± 0.01	two annuli tested
commercial nylon washer	0.05 ± 0.02	
PC	0.11 ± 0.01	specimen shattered
Noryl	0.09 ± 0.02	
PVDF	0.14 ± 0.01 0.14	two annuli tested
copper	0.19 ± 0.02	
copper lubricated by gun barrel oil	0.13	
nylon washer	0.04	silicone grease lubricant
nylon washer	0.035 ± 0.005 0.015 ± 0.005 0.005 ± 0.005	gun barrel lubricant, three specimens tested
nylon washer	0.0 0.0	two specimens tested petroleum jelly lubricant

An approximate relation between the coefficient of friction μ and the friction parameter m was found by Male & Depierre (1970) to be

$$\mu = m/(2\sqrt{3}) \tag{6}$$

although a comparison of Avitzur's analysis for an annulus with a hole of zero radius (i.e. a solid cylinder) with an analysis for a cylinder with a constant coefficient of friction over the interface suggests the relation (Gorham *et al.* 1984)

$$\mu = m/\sqrt{3}. \tag{7}$$

Some aspects of the behaviour of petroleum jelly, when used as a lubricant for solid discs, can be seen in the sequence presented in figure 11, plate 7, of a 1 mm thick PC specimen. The lubricant is seen as a pattern of smears, which initially extend within the area of the disc. After 14 μs the smear pattern has disappeared around the periphery, but is still visible in the centre where the specimen is presumably concave. The disc expands without jetting of lubricant until it fails catastrophically about 240 μs after impact at a strain of 1.15. After this, streaks of lubricant can be seen moving radially outwards from the edge of the specimen. Explosive fracture of PC seems to be a feature of thin specimens, for although failure of 2 mm thick discs is rapid, the specimen boundary does not move as fast as in figure 11, where the speed was *ca.* 250 m s^{-1}. It should be noted here that photographic sequences of the failure of injection-moulded PC discs obtained in this laboratory (figures 5 and 11, and in Swallowe *et al.* 1986 and Walley *et al.* 1985) do not show any obvious relation between the place where failure initiates and the point of injection into the mould (the gate). In one case (2 mm thick disc, not shown) failure started at the gate, but in Swallowe *et al.* (1986), shear initiated *opposite* the gate. In the other three cases, the failure points lay at intermediate positions.

In summary, high-speed photography revealed the behaviour of these materials under conditions of high strain rates out to large strains, showed the development of discolouration of heat-sensitive film placed in contact with deforming specimens, and allowed quantitative measurements of the friction under dynamic loading.

4. Stress–strain curves at three different strain rates

(*a*) *Preliminary remarks*

It is not possible to specify a unique value of, say, the flow stress for a given polymer as it varies according to the grade of material and also with the history of a given batch (Ashby & Jones 1986). Thus tables of polymer properties usually give a range of values. So if any trend in behaviour is to be seen from low strain rates to high strain rates, measurements must be made on specimens from the same batch, reasonably close together in time. In the experiments reported below, the work was completed within a three month period, the nylons, PC, and Noryl specimens having been injection moulded some eleven months beforehand and the PBT and PVDF about two months beforehand. Also it is well known that friction on the end faces of the discs can have a substantial effect on the measured value of the yield stress. Gorham *et al.* (1984) gave the following expression for the magnitude of the friction correction:

$$p = (1+2ma/(3\sqrt{3}h))\,\sigma_y, \tag{8}$$

where p is the measured mean pressure, a the specimen radius, h the specimen height, and σ_y the material yield stress. It can be seen that the measured stress depends not only on the friction parameter m but also on the ratio a/h. Two cases can be considered. (*a*) Where $m = 0$. For perfect lubrication, no correction needs to be made, and the measured stress–strain curves should be *independent* of a/h. End effects are unimportant. (*b*) Where $m > 0$ and known. If the magnitude of the friction is known, the correction of equation (8) can be applied. It would not be necessary for a/h to be the same for all specimens tested, especially as m takes different values at the various strain rates used, but it is good practise to compare geometrically similar specimens. This was done for most of the experiments on those polymers that were tested at all strain rates, a/h being set equal to 1.25/1. Exceptions are noted where they appear.

(*b*) *Low strain rates* (*ca.* 10^{-2} s^{-1})

These were imposed with an Instron mechanical testing machine. A tension–compression cage was modified to take the toughened glass anvils used in the high-speed photography experiments. An optical arrangement identical to that shown in figure 1 was set up. In addition, displacement transducers were attached to the anvils with metal plates. Two were positioned on opposite sides of the anvils so as to cancel out any effects due to bending. Attaching transducers to the anvils overcomes inaccuracies due to softness of the machine or hysteresis of the compression cage. The outputs of the load cell and the displacement transducers were logged by using a microcomputer. This was also used to operate the shutter and autowind of a camera so that a visual record of the deforming specimen was obtained. Thus it was known what the force and longitudinal compression were when each picture was taken. One other difference from the high-speed case was that the glass anvil surfaces were ground flat, the surface finish having a profile whose peaks and troughs were about 1 μm apart in height. The reason this was done was to provide lubricant trapping sites to try and prevent seizing (Gorham *et al.* 1984). Lead washers were used to protect the rear surface of the glass from the machined steel surface of the compression cage. When the system was loaded up to a force of 4 t, the transducers registered a compression of 20 μm compared to the reading when the force started to rise as the anvils made contact. The maximum load any polymer disc was loaded to was *ca.* 2 t, at which the deflection was *ca.* 10 μm. So to enhance the accuracy of the yield stress values, the zero level was offset by 10 μm relative to the point where the anvils first contact.

The ring test was again used to determine the friction and to identify a suitable lubricant. The photographic record could be used, as in the rapid deformation studies, or measurements could be made on recovered specimens. In each case, the longitudinal strain could be computed either from the area (assuming volume conservation) or directly from the thickness. Two lubricants were investigated with nylon 6: petroleum jelly and candlewax (figure 12). It is clear that the higher-molecular-mass hydrocarbon worked better, having a higher viscosity and hence not so subject to being squeezed out, but even so it did not reduce the friction to zero. Being transparent, however, it was adopted for these experiments rather than the possible alternatives of molybdenum disulphide or graphite. One other lubricant was tried with copper, namely PTFE applied with a spray, but it was found to have very little effect. Values of the friction parameter m for the various materials with and without lubricants are presented in table 4. 'Dynamic' refers to values computed from the record of the deforming specimen, 'recovered' refers to values computed from the recovered specimen. It can be seen that the

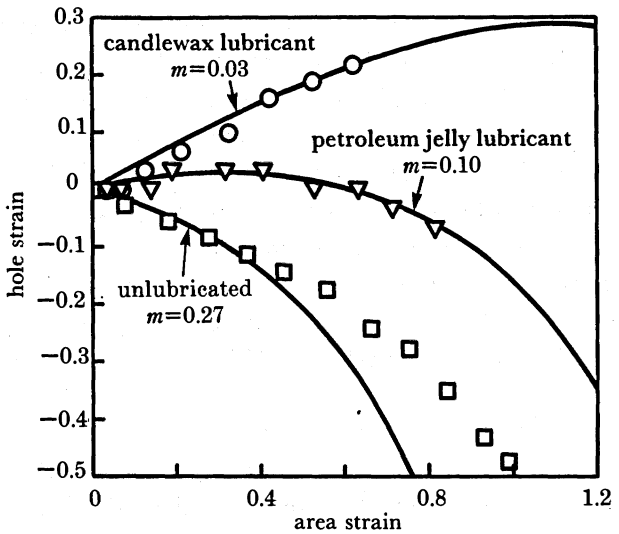

FIGURE 12. Avitzur plots of dry N6 annuli (dimensions given in figure 9) deforming in an Instron between glass anvils with and without lubricant. Candlewax can be seen to be a better lubricant than petroleum jelly at this strain rate, although not perfect. The Avitzur analysis does not work well for the unlubricated case. Symbols: ○, candlewax lubrication; ▽, petroleum jelly lubricant; □, unlubricated.

TABLE 4. VALUES OF AVITZUR'S FRICTION PARAMETER, m, FOR VARIOUS MATERIALS DEFORMED IN AN INSTRON MACHINE BETWEEN GLASS ANVILS

material	lubricant	dynamic from thickness measurement	dynamic from area measurement	recovered from thickness measurement	recovered from area measurement
dry N6	none	0.27 ± 0.03	0.27 ± 0.03	0.25	0.22
dry N6	petroleum jelly	0.10	0.10	0.13	0.12
dry N6	candlewax	(*a*) 0.06	0.06	0.065	0.065
		(*b*) 0.03	0.03	0.065	0.065
wet N6	none	0.4	0.4	0.21	0.20
dry N66	none	deviates from Avitzur's analysis	0.20	0.22	0.20
dry N66	candlewax	0.04	0.04	0.08	0.08
wet N66	none	0.3	0.3	0.23	0.21
wet N66	candlewax	—	—	0.06	0.06
PC	none	(*a*) 0.4	0.4	0.29	0.27
		(*b*) 0.4	0.4	0.27	0.23
PC	candlewax	(*a*) 0.1	0.10	0.07	0.07
		(*b*) 0.12	0.12	0.07	0.07
Noryl	none	deviates from Avitzur's analysis	0.3	0.27	0.23
Noryl	candlewax	disc data not recoverable	*ca.* 0.12 (hole seized)	0.085	0.085
PBT	none	0.20	0.25	0.145	0.225
PVDF	none	(*a*) 0.15	0.17	0.19	0.19
		(*b*) 0.17 ± 0.03	0.25	irregularly deformed specimen	
PVDF	candlewax	0.08	0.08	0.08	0.095
copper	none	0.25 ± 0.05	0.27 ± 0.03	0.27	0.29
copper	PTFE	0.20	0.27 ± 0.03	irregularly deformed specimen	

frictional stress of the unlubricated polymers is considerably higher in the Instron tests than in the dropweight experiments. This is probably because of the roughness of the glass, and to the absence of a rapidly shearing surface layer.

A test of the theory was made by deforming 1 mm and 2 mm thick solid discs of some of the polymers with and without lubricant. An example of the stress–strain curves from which the flow stresses (or in the case of nylon 66, the proof stress at a strain of 0.1) are taken are given in figure 13. Three polymers were chosen for the test on the basis of their stress–strain curves and the accuracy with which m could be determined for them, namely dry nylon 66, PC and PVDF. The ratios of the measured flow stresses were calculated and compared to that predicted by equation (8). The values of m used may be found in table 4. The values of the flow stresses used, their ratios, and various predicted ratios are given in table 5. It can be seen that equation (8) usually underestimates the measured ratios, though the Avitzur theory is closer than the empirical relation found by Male & Depierre (1970) for metals. Briscoe & Nosker (1984) have pointed out that the von Mises yield criterion, which is the basis of Avitzur's analysis, is not the best yield criterion for polymers as it does not take into account the pressure sensitivity of the yield process. They showed that the pressure-modified Tresca criterion introduces a term $(1-2\alpha)$ into the denominator of their friction expression, where α is the pressure sensitivity of the shear yield stress. However, use of the value for α of 0.07 ± 0.01 for

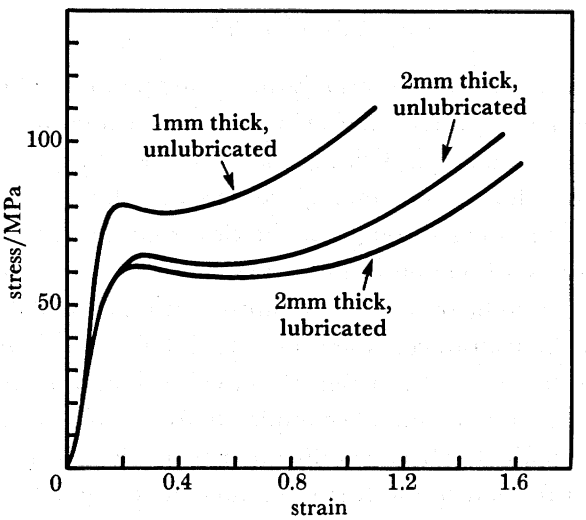

FIGURE 13. Compressive stress–strain curves for PVDF obtained by using an Instron with glass anvils and calculated from the transducer outputs. The discs were all 5 mm in diameter. The effects of thickness and lubrication conditions are clearly seen. Each curve is an average from two separate experiments.

TABLE 5. A COMPARISON OF THEORY AND EXPERIMENT FOR THE FRICTION OF POLYMERS DEFORMED BETWEEN GLASS ANVILS AT A LOW STRAIN RATE (10^{-2} s^{-1})

	stress close to the yield strain/MPa			ratios					
				A/B			B/C		
material	1 mm thick, unlubricated $= A$	2 mm thick, unlubricated $= B$	2 mm thick, candlewax lubricant $= C$	measured	predicted $\mu = \frac{1}{\sqrt{3}}m$	predicted $\mu = \frac{1}{2\sqrt{3}}m$	measured	predicted $\mu = \frac{1}{\sqrt{3}}m$	predicted $\mu = \frac{1}{2\sqrt{3}}m$
dry nylon 66	100	92	81	1.09	1.13	1.07	1.14	1.11	1.05
PC	106	75.7	63.8	1.40	1.24	1.08	1.19	1.07	1.06
PVDF	80.6	69	66.6	1.17	1.15	1.09	1.04	1.07	1.02

PC given in Briscoe & Smith (1981) does not substantially change the ratios A/B and B/C (where A, B and C are defined in table 5). It is doubtful too whether the interfacial shear stress remains constant during deformation. The plots of annuli deformation presented in figure 12 deviate from Avitzur curves at a longitudinal strain of *ca.* 0.4, the hole closing up faster than theory predicts, implying an increase in friction to some unknown value. Thus although it may be possible to correct the tabulated values of flow stress for friction, it is not possible as yet to correct the stress–strain curves over their whole range, and hence the stress–strain curves presented later in figure 16 have not been corrected for friction.

Equation (8) predicts that using thicker specimens decreases the effect of friction on the measured stress, and this is borne out by the results in table 5. Specimens of thickness 2 mm lubricated by candlewax were therefore used to give measurements closest to the intrinsic yield stress. One problem, though, is that the lubricant introduces an inevitable error due to its thickness. This was measured *in situ* with the displacement transducers, and usually lay in the range 10–15 μm on each face. This cannot easily be corrected for, as the lubricant film will thin down in an unpredictable manner as the deformation proceeds.

Another error in the thickness measurement is due to elastic indentation of the anvils. Glass was chosen as anvil material for its transparency, but it is more compliant than the hardened steel normally used as an anvil material. Timoshenko & Goodier (1970) give the following formula for the depth of an elastic indentation δ of a semi-infinite half-space by a punch,

$$\delta = F(1-\nu^2)/2RE, \tag{9}$$

where F is the applied force, ν the Poisson ratio, E the Young modulus of the indented material, and R the radius of the punch. In these experiments, the correction to the specimen thickness is 2δ as two anvils are being indented. Taking ν as 0.25 and E as 75 GPa for the glass, the typical size of this correction for the polymer specimens was 10 μm.

The correction can be computed throughout the deformation as the photographic record gives the radius of the disc as a function of time. The effect of this correction may be judged from figure 14. It can be seen to be of small effect until a strain of *ca.* 0.6 is reached. The value of the strain measured by the transducers then starts to differ considerably from that deduced from the photographs, the diametral strain being less than it should be were volume conserved. The indentation formula is seen to be unable completely to explain the discrepancy: the curve corrected for indentation usually lay between the other two. The effect is most marked for PC, which also has the highest friction of the (dry) polymers investigated. The most likely origin of the discrepancy is compression of the material because of the hydrostatic pressure generated by the applied load combined with the interfacial frictional shear stress. For consider the stress–strain graph for an unlubricated specimen of PC 2 mm thick (figure 15). At a stress level of 320 MPa, the strain according to the photographic record is 1.1, whereas the strain measured by the transducers (and corrected for indentation) is 1.2. This implies a volume strain of 0.095. The bulk modulus K of PC is almost equal to the Young modulus as its Poisson's ratio is 0.31 (Whitney & Andrews 1967) i.e. *ca.* 2 GPa (see Shell Chemicals *Physical and Chemical properties of polymers and moulding compounds*). The frictional stress τ can be considered to be a radial compressive stress acting at the edges of the boundaries of the top and bottom surfaces of magnitude $m\sigma/\sqrt{3}$ where σ is applied stress (here 320 MPa). For sufficiently thin specimens, we may ignore the variation of the radial stress through the thickness of the specimen, and hence the hydrostatic pressure (the trace of the stress tensor) is $\frac{1}{3}(\sigma+2\tau)$. Taking m as 0.4 the

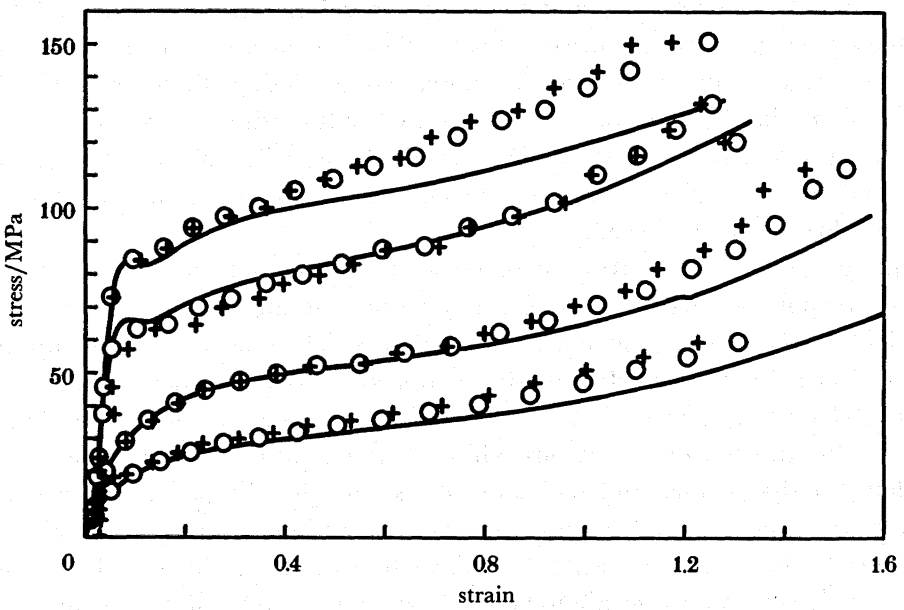

FIGURE 14. Comparison of Instron stress–strain curves for the two nylons computed from displacement transducer outputs (solid lines) with the values of stress and strain calculated from photographic records. The + symbol is *without* indentation correction, the o symbol is *with* indentation correction. All specimens were lubricated with candlewax and were 2 mm in thickness, 5 mm in diameter.

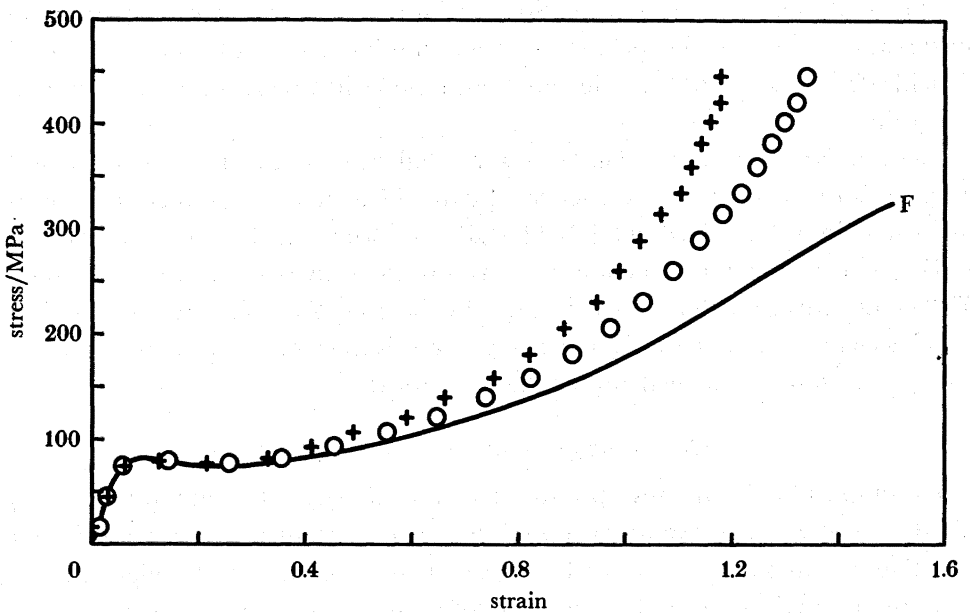

FIGURE 15. Instron stress–strain curve for an unlubricated PC specimen ($d = 5$ mm, $t = 2$ mm) showing large discrepancies between stress–strain curves computed from the transducer output and the values calculated on the basis of the photographic record. This suggests that volume is not conserved during plastic flow in this case. F marks fracture. The symbols + and o have the same meaning as in figure 14.

hydrostatic pressure P is then 130 MPa. This will give a volume strain P/K of *ca.* 0.07, which is in reasonable agreement with the measured value. Direct measurements on volume changes in uniaxial compression have been made by other workers using dilatometry (Whitney & Andrews 1967; Pampillo & Davis 1971). They showed that plastic deformation of PC results in a volume change greater than that predicted on the basis of Poisson's ratio i.e. that plastic flow does not take place at constant volume. The effect was, however, small: a volume change of *ca.* 0.3 % after loading to 80 MPa.

Figure 16 presents compressive stress–strain curves for all the polymers (and copper) tested in the Instron. The polymer specimens were 5 mm in diameter and 2 mm in thickness with the exception of PTFE, and were lubricated with candlewax. These curves were computed from the transducer record, and no correction has been applied for friction. They are thus inaccurate at large strains (0.8 or more). The effect of moisture on the mechanical properties of the nylons is very marked. The water-saturated nylons exhibit a more gradual changeover from elasticity to yielding than the dry nylons, and their flow stresses are nearly halved. PC was found to fracture in the same manner as in the dropweight experiment, and at almost the same diametral strain: 1.15 ± 0.05 (calculated from three lubricated specimens). The transducers recorded the compressive fracture strain to be 1.4 ± 0.1 (figure 16*a*). All the polymers, with the exception of the water-saturated nylons and PTFE, showed a yield drop. In some this was sudden (within a strain increment of 0.1): PC, dry nylon, Noryl. In some, it was more gradual: PVDF, PBT. Water-saturated nylons and PTFE showed monotonically increasing stress against strain curves. Unloading was also measured, though not down to zero stress levels. PC showed the most amount of recoverable strain, up to 0.2 at a strain of 1.3. This probably accounts for the great violence of its failure. Stress–strain curves are also presented for copper. The gun lubricant did not alter the yield stress much, but it did raise the stress level at a given strain after yield. PTFE lubricant spray lowered both the yield stress and the subsequent stress level at any strain.

An experiment where PC discs were compressed unlubricated one after the other showed a drop in fracture strain down the sequence (figure 17), the values measured from the photographs being (in order): 1.18, 0.88, 0.82, 0.81, and from the displacement transducers: 1.5, 1.15, 1.07 and 1.0. This phenomenon we attribute to an increase in friction because of a build-up of polymer films on the anvils. It can also be seen that the stress levels rise more rapidly for each successor in the series. These two observations seem to imply that failure occurs when an initial *stress* state is reached rather than a critical strain.

(*c*) *Medium-range strain rates* (*ca.* 10^3 s^{-1})

Strain rates comparable with those produced in the high-speed photographic apparatus were investigated with an instrumented dropweight machine (figure 18) (see also Heavens & Field 1974). The specimen is compressed between two hardened steel rollers 12.7 mm in diameter. The upper anvil is struck by a weight (of mass 2.4 kg in these experiments) raised to a height of *ca.* 30 cm. The speed of impact is measured using the voltage output of a tachometer coupled to the weight by a fine steel wire. A speed of impact of 2.3 m s^{-1} was usually obtained, giving a nominal strain rate of 10^3 s^{-1} for a 2 mm thick disc. The compression of the lowest roller (r1) was measured by using two resistance strain gauges positioned across a diameter. Their output was recorded by using a Datalab Transient Recorder. A spring-steel washer was inserted between rollers r1 and r2 so that the instrumented roller (r1) was

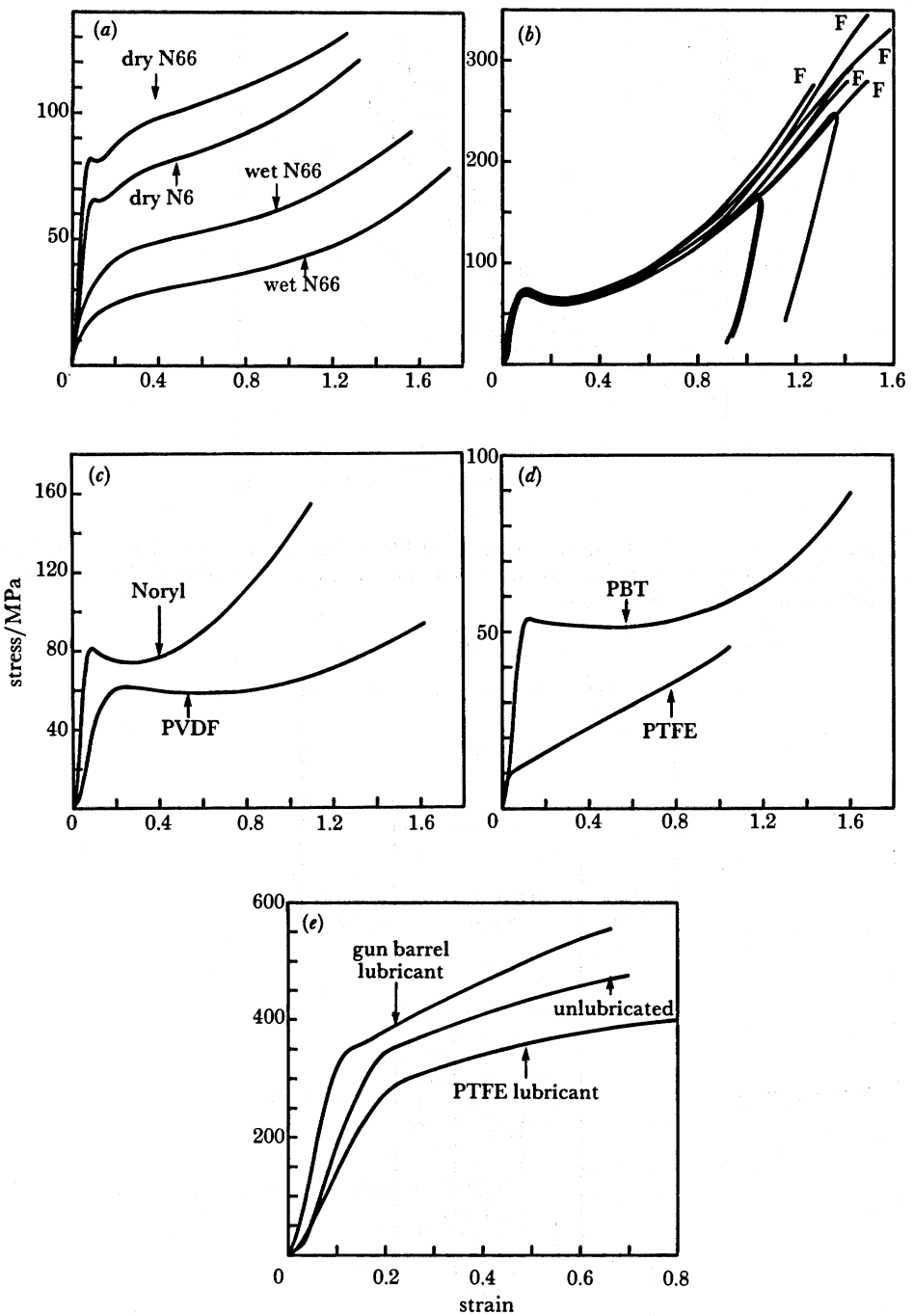

FIGURE 16. Instron stress–strain curves obtained from 5 mm diameter, 2 mm thick lubricated discs of polymers and 6.5 mm diameter, 1 mm thick discs of copper. The curves are plotted directly from the transducer outputs with no correction for indentation or friction, and so are inaccurate for strains 1.0 or greater, depending on the material: (*a*) wet and dry N6 and N66; (*b*) PC (F marks fracture). Note the large degree of elastic recovery in unbroken specimens; (*c*) Noryl and PVDF; (*d*) PBT and PTFE; (*e*) copper, lubricated and unlubricated. Curves from repeat experiments are included in (*b*) giving an idea of the reproducibility.

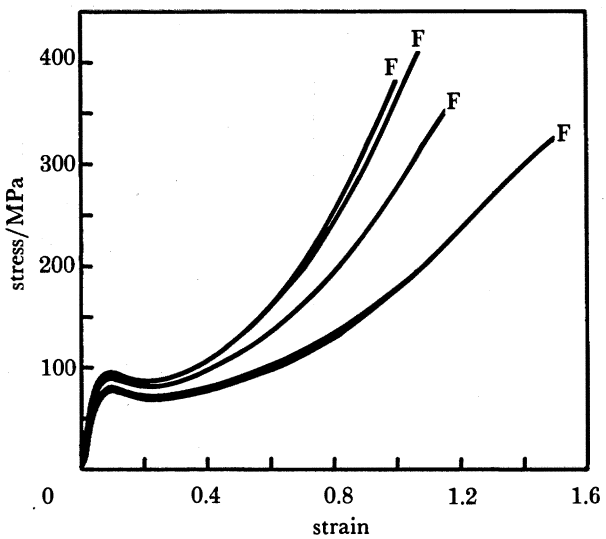

FIGURE 17. Instron stress–strain curves obtained from a set of PC specimens (2 mm in thickness, unlubricated) compressed one after the other without cleaning the anvils. The failure strain *decreases* with successive members of the sequence, because of increasing friction.

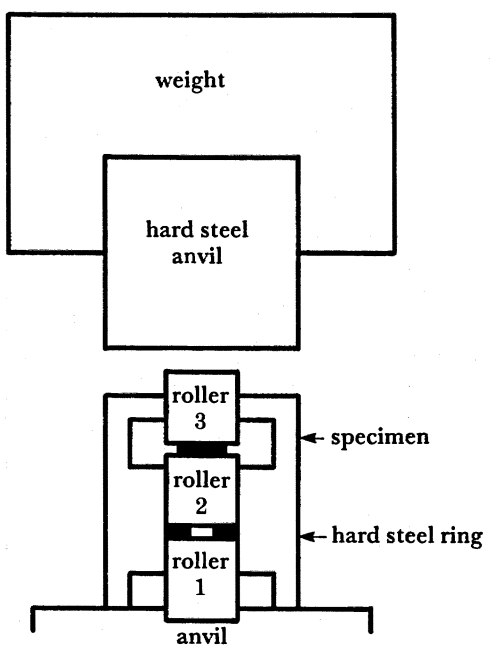

FIGURE 18. Schematic diagram of the instrumented dropweight apparatus.

compressed most on its periphery rather than its centre (which is inaccessible to instrumentation). The calibration factor and an empirical expression for the compressibility of the system when loaded by a known force were determined from direct impacts with no specimen present. Care had to be taken that the electrical instrumentation did not form an inductive loop around the rollers, as the dropweight is made of mild steel and its fall generates spurious EMFs (electromotive forces).

Another mechanical correction that was found to be necessary was that for the centre of mass motion of the rollers and specimen. This arises because the blacksmith's anvil on which they rest, although massive (*ca.* 80 kg), is not infinite in mass. Thus even when the force measured by the strain gauges has fallen to zero, the dropweight is still moving downwards. With these extra corrections the generation of stress–strain curves proceeds according to the analysis of Heavens & Field (1974), which assumes that the rollers deform quasi-statically and that therefore the displacement–time curve is given by numerically integrating the force–time data twice by using the values of the dropweight mass and its impact speed. The strain is then given by equation (1). The stress is the force divided by the current area, which is calculated from the height displacement assuming volume conservation. The specimens used in this apparatus were the 2 mm thick, 5 mm diameter injection moulded discs. Lubrication (when used) was provided by petroleum jelly. Unfortunately it proved not to be possible to obtain sufficiently accurate uniaxial loading to obtain friction parameters for the polymers: annuli deformed elliptically especially with lubricant present. Values of m were, however, obtained for copper, these being 0.21 (unlubricated) and 0.09 (with the gun barrel lubricant). These measurements were made on recovered specimens. That friction is important in this system can be seen from the graphs presented in figure 19, where (with the exception of dry nylon 6) the measured stress for unlubricated specimens is usually some 20 MPa higher than for those specimens lubricated by petroleum jelly. As the diameter of the rollers is 12.7 mm, the maximum strain for which these curves is valid is 1.85 for 5 mm diameter specimens. The original stress–strain curves show regular oscillations due to the rollers being set into vibration by the impact. The curves in figure 19 are the averages of several separate experiments.

Because of the inevitable slight non-planarity of the impact of the weight, the polymer discs were sometimes squeezed out in one direction during deformation, particularly if lubricated. This departure from the ideal case of uniaxial compression will lead to errors in the stress–strain curves, especially at large strains. This effect was most marked for dry N6, where the stress levels drop continuously until unloading takes place. However, a reasonably close approximation to uniaxial loading was often obtained, as can be seen from photographs of recovered specimens of dry N66 and PC (figure 20, plate 8). This figure also shows the failure mode we often observed for the nylons when subjected to tensile or hoop stresses, in this case caused by material overflowing the edge of the anvils. Partial failure of PC by shear banding rather than 'explosive' fragmentation was usually obtained in this apparatus, probably because the energy available is only just enough to cause fracture. This is borne out by the fact that it was not possible to take 2 mm thick specimens to failure under the conditions of impact given at the beginning of this section: thinner specimens (1.5 mm and 1.0 mm thick) had to be used. Although this apparatus is probably the least accurate of the three used, fracture strains were calculated for essentially the same value as found by using an Instron and the high-speed photography apparatus, bearing in mind that the strains calculated are true height strains rather than area strains. Two 1.5 mm thick unlubricated specimens fractured at strains of 1.2 and 1.4. Three 1.0 mm thick unlubricated specimens failed at strains of 0.9, 1.0, and 1.0. This gives us confidence that the stress–strain curves obtained from thus apparatus have been calculated correctly.

(*d*) *High strain rates* (*ca.* 10^4 s^{-1})

The highest strain rates of all were produced in a miniaturized direct impact Kolsky bar (Gorham 1980). This system has recently been modified to determine the strain directly from

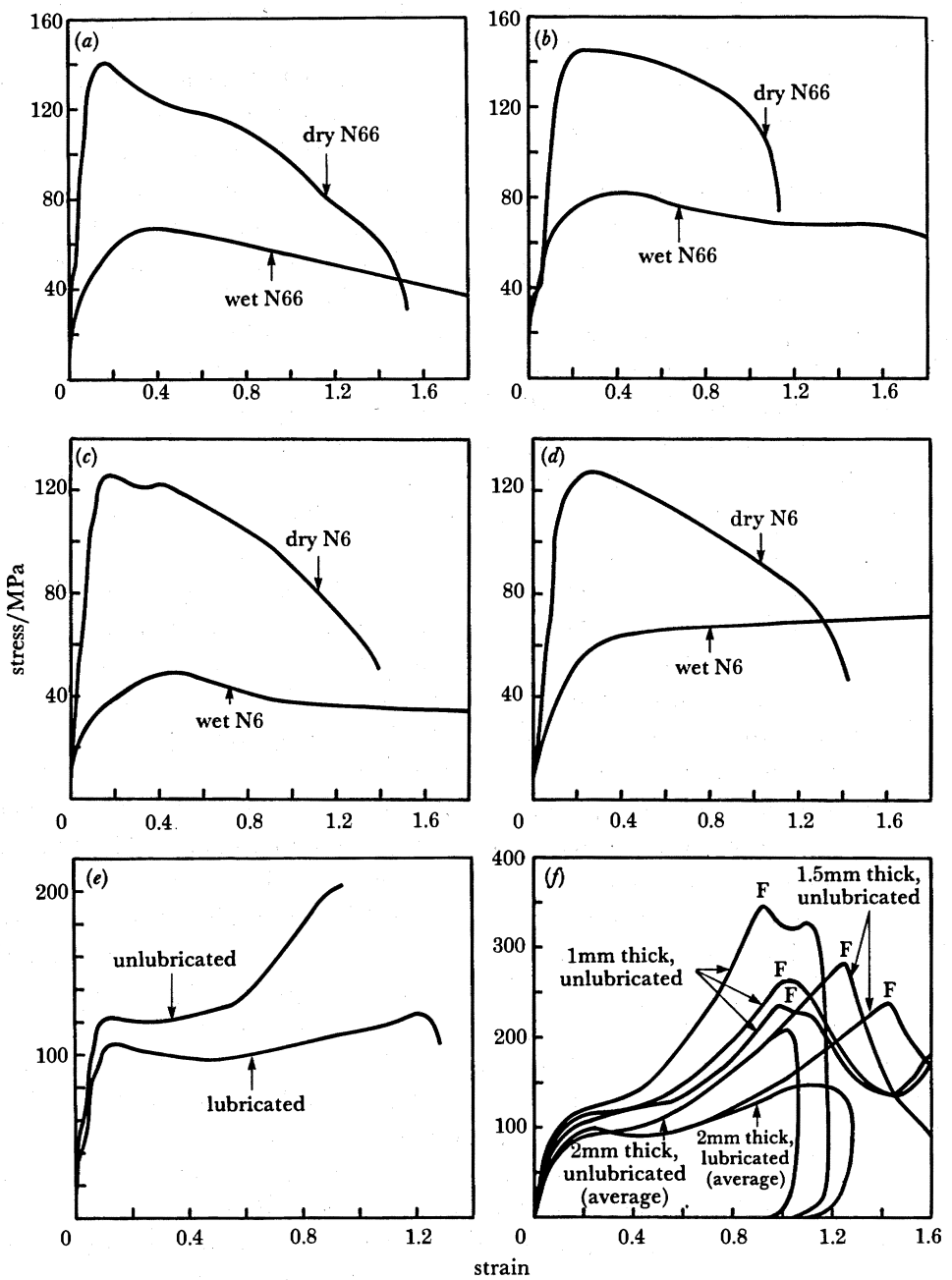

FIGURE 19*a–f*. For description see opposite.

force–time measurements (Pope & Field 1984) in a manner analogous to the dropweight, though because the output bar is long (150 mm as opposed to 25 mm) and the experiment duration short (30 μs as opposed to *ca.* 500 μs), stress equilibrium does not obtain. In instrumentation terms, the Kolsky bar is excited *above* and the dropweight rollers are excited *below* their respective resonant frequencies. The method of calculating the strain again assumes volume conservation, and also that the bar-specimen system can be treated by one-dimensional wave propagation theory. The compression of the specimen is then determined by the speed

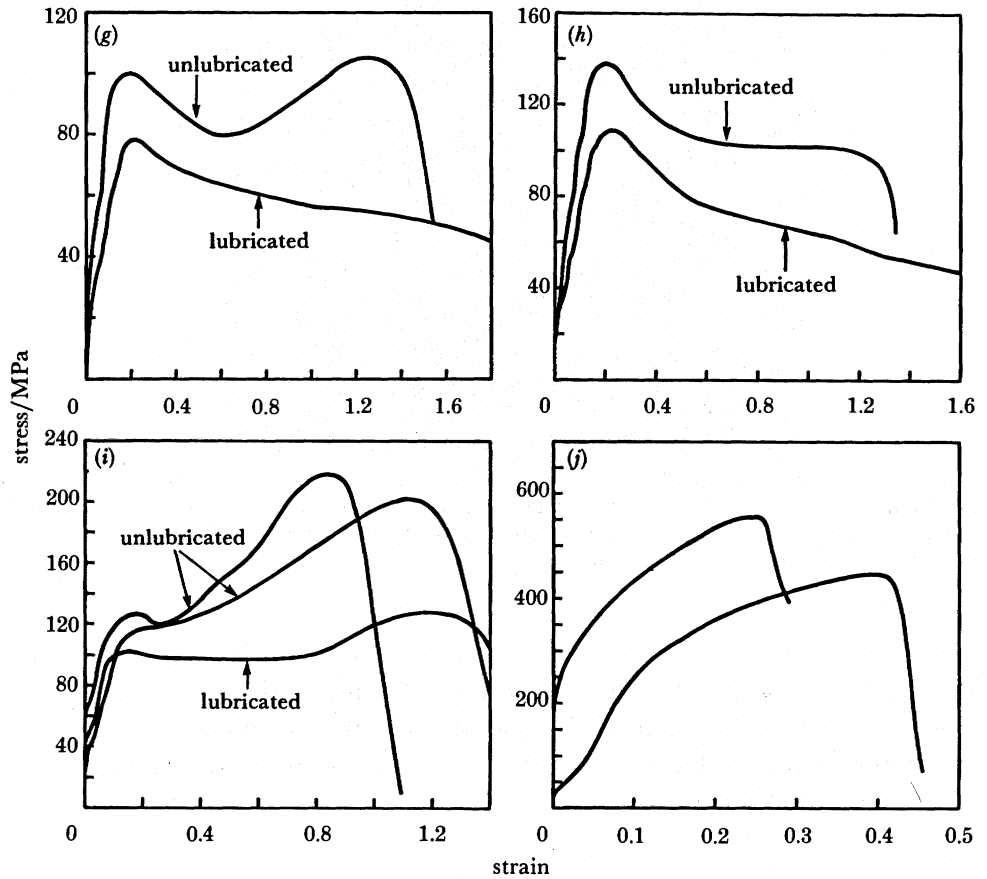

FIGURE 19. Stress–strain curves for various polymers and copper obtained in the dropweight machine of figure 18. The polymers had dimensions 5 mm diameter and 2 mm thickness (unless otherwise specified). The lubricant (where used) was petroleum jelly. (*a*) N66 wet and dry, lubricated; (*b*) N66 wet and dry, unlubricated; (*c*) N6 wet and dry, lubricated; (*d*) N6 wet and dry, unlubricated; (*e*) Noryl, lubricated and unlubricated; (*f*) PC, 1.0 and 1.5 mm thick unlubricated discs, and 2.0 mm thick discs, lubricated and unlubricated. F marks fracture; (*g*) PBT lubricated and unlubricated; (*h*) PVDF, lubricated and unlubricated; (*i*) PES, lubricated and unlubricated disc 6.5 mm diameter, 1 mm thick; (*j*) copper (dimensions given in figure 16), lubricated by gun barrel oil and unlubricated. Each curve is an average of two separate experiments except for those PC specimens that fractured.

of impact v, and the mechanical impedances Z ($= A\sqrt{\rho E}$) of the striker and output bars, where A is the cross-sectional area, ρ the density, and E the Young modulus, by the expression

$$h(t) = h_0 - vt + \frac{(Z_1+Z_2)}{Z_1 Z_2}\int_0^t f(t')\,\mathrm{d}t', \tag{10}$$

where h_0 is the original height, h the height at a time t, and $f(t)$ the measured force pulse. The impedances of the striker and output bars are determined directly by performing an impact with no specimen present. The semiconductor strain gauges then record a signal consisting of a compressive wave of duration $2l_1/c_1$ where l_1 is the length and c_1 is the wave speed of the striker bar, followed by a tensile wave that returns after a time $2l_2/c_2$ where l_2 is the distance from the gauges to the far end of the output bar and c_2 is the wave speed in the striker bar (figure 21). Knowing the mass and length of the bars their densities may be calculated, and because $c = \sqrt{(E/\rho)}$ the impedances of the two materials may be calculated as being ρc. Two

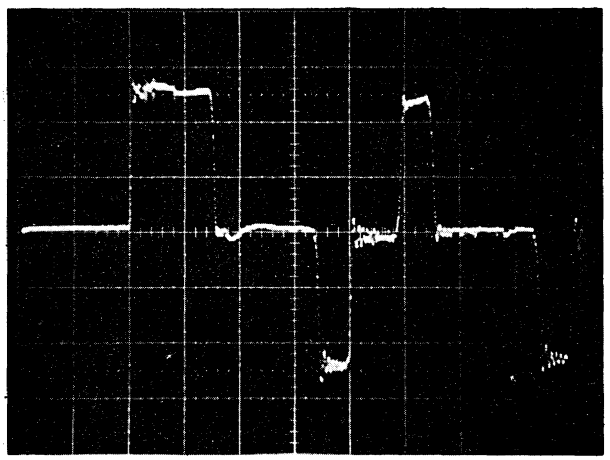

FIGURE 21. Strain gauge output from direct impact of 75 mm long silver steel rod 3 mm in diameter on WC output bar, 213±2 mm long and 3.17 mm in diameter. The length of the initial compressive pulse gives the impedance of the striker. The time from the beginning of the compressive pulse to the return of the first tensile pulse gives the impedance of the output bar (see table 6).

different combinations of striker and output bars have been used (Ti alloy on W alloy, and silver on WC) and their properties are given in table 6. The consistency of the method was checked using these two combinations to test high-density PE, a medium-density PE (as used in gas-distribution systems; Walley & Field 1987), and an extrusion grade of Noryl (figure 22). The agreement is seen to be close.

TABLE 6. MECHANICAL IMPEDANCES OF THE MATERIALS USED IN THE DIRECT IMPACT KOLSKY BAR

material	density / kg m^{-3}	wavespeed / km s^{-1}	impedance / kg m^{-2} s^{-1}
Ti alloy striker	4400	4.91	2.16×10^7
silver steel striker	7750	5.18	3.99×10^7
tungsten alloy output bar	16840	4.47	7.53×10^7
tungsten carbide output bar	14900	6.22	9.27×10^7

The majority of specimens derived from injection moulded discs were 2.5 mm in diameter and 1 mm thick. A leather punch or a flat ended punch was used to cut them out of discs or sheet. Specimens of very brittle polymers such as Perspex (PMMA), or very tough polymers such as PC, could not be prepared using a leather punch, though this tool produced less deformation where it could be used (the flat-ended punch tends to produce specimens that are trapezoidal in cross section). Stress–strain curves obtained from specimens formed using a leather punch showed much less scatter than those prepared using a flat-ended punch. Figure 23 shows also that the absolute value of the flow stress can be affected by the method of preparation. This effect was most marked for PBT, though the curves obtained for PVDF were relatively insensitive to the tool used.

By contrast, most of the specimens derived from sheet or rod were 2 mm in diameter. All

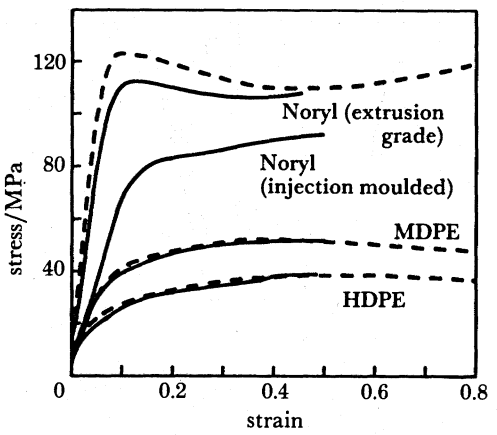

FIGURE 22. Stress–strain curves obtained with the direct impact Kolsky bar to show the consistency of the calculation method with two combinations of striker and output bars and also the variation in flow stress with grade of polymer. The dotted lines were obtained with a 70 mm long Ti alloy striker on a W alloy output bar. The solid lines were obtained with the silver steel projectile on the WC output bar. The stress–strain curves obtained with the silver steel and WC combination terminate at smaller strains because the impact speeds used were lower (to avoid the risk of chipping the WC bar) and hence the strain achieved in the time the wave analysis is valid (30 μs) is less. Two of the polymers were tested (extrusion grade Noryl and HDPE) by using specimens with an a/h ratio of 1/1 rather than 1.25/1. The grade of polymer tested can be seen to be important even at these very high strain rates.

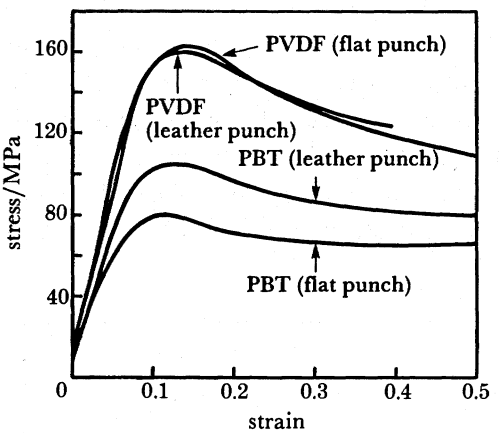

FIGURE 23. Comparison of Kolsky bar stress–strain curves obtained from PBT and PVDF specimens prepared by the two different methods (flat punch and leather punch).

were 1 mm thick with the exception of PTFE (0.8 mm) and MDPE (0.75 mm). In addition, two polymers were available in very thin sheet (*ca.* 0.5 mm thick): PVC and cellulose acetate. Some 1 mm diameter specimens were therefore made from such sheet in order to attain higher strain rates. The stress–strain curves for PVC are the same within experimental error for both sorts of specimens. But cellulose acetate shows a stress enhancement for the smaller specimens, which also fail at a strain of 0.5. It is possible the difference may be due to lubricant breakdown, as the stress can be seen to rise rapidly after a strain of *ca.* 0.3 in a manner characteristic of high friction conditions (figure 24).

Lubrication was by petroleum jelly (with the exception of some of the experiments on extrusion grade Noryl and polyethylene where the lubricant used was the one reported by

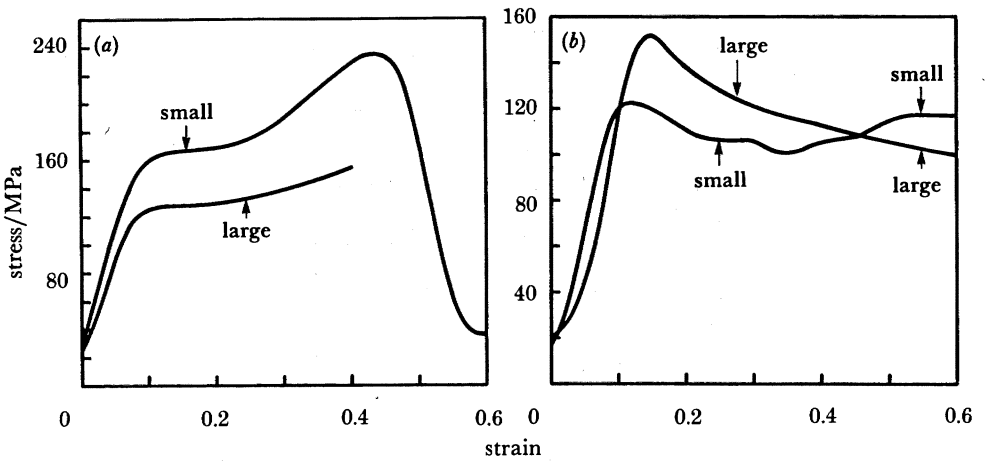

FIGURE 24. Stress–strain curves obtained for two different size specimens of: (*a*) cellulose acetate; (*b*) PVC. The larger cellulose acetate specimens had dimensions 2.0 mm diameter, 1.1 mm thick; the smaller CAc specimens had dimensions 1 mm diameter, 0.5 mm thick. The larger PVC specimens had dimensions 2 mm diameter, 0.6 mm thick; the smaller specimens had dimensions 1 mm diameter, 0.5 mm thick.

Gorham *et al.* (1984) as giving the lowest friction and most reproducible conditions for experiments on metals). Thus we may assume that the friction is initially zero, and hence the aspect ratio of the specimens should have no effect.

It was shown in Gorham *et al.* (1984) that there is no specimen geometry for which inertia is identically zero. The argument has been refined and developed further in Pope (1986) and the resulting expressions used to calculate the magnitude of the inertial stresses for a conventional Hopkinson bar and the miniaturized direct impact Kolsky bar for polymer specimens over a range of strain rates (figure 25). It can be seen that inertial stresses are negligible in our apparatus even at strain rates of $10^4\ s^{-1}$, and this is because very small

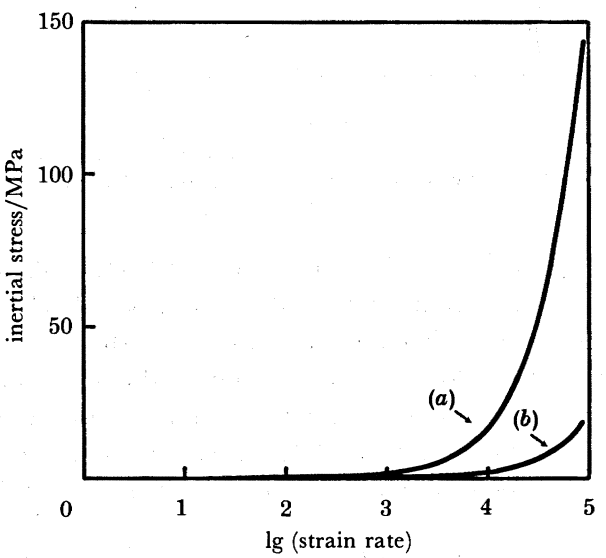

FIGURE 25. Comparison of inertial stresses for polymer specimens of size typical of (*a*) a conventional Hopkinson bar as opposed to (*b*) our miniaturized direct impact Kolsky bar.

specimens are used. Stress–strain curves obtained with this system are presented in figure 26. Several polymers were tested at this strain rate in addition to the ones deformed at the two lower strain rates. The dry nylons and ABS deform at constant flow stress. The wet nylons, PES, PC, and particularly PTFE, show monotonically increasing stress–strain curves whereas PBT and PVDF show yield drops. Two brittle polymers, PS, and PMMA fail at strains of *ca.* 0.1. The curves are drawn until either the strain is reached at which material starts to overflow the bars, which in some cases is $2\ln(\frac{3}{2.5}) = 0.4$ and in others $2\ln(\frac{3}{2}) = 0.8$, or the time is reached when the wave that travels up the impact bar returns (30 μs). The specimens go on deforming long after this, of course. Those that were made of polymers such as PTFE, shatter, but many of those made of other polymers can be recovered. Wet N6 generally is punched right through forming rings whereas wet N66 and both nylons in the dry state are recovered with cracking due to tensile hoop stresses. Table 7 presents the values of the flow stresses at the three rates of strain that were studied. It can be seen that all the polymers that were investigated show an increase in yield (or flow) stress in going from the low strain rates obtainable in an Instron to the higher rates achievable in the drop-weight or Kolsky bar machines. Some, such as N6, PVDF, and PBT, show at least a factor of two increase in their yield stress. Others, such

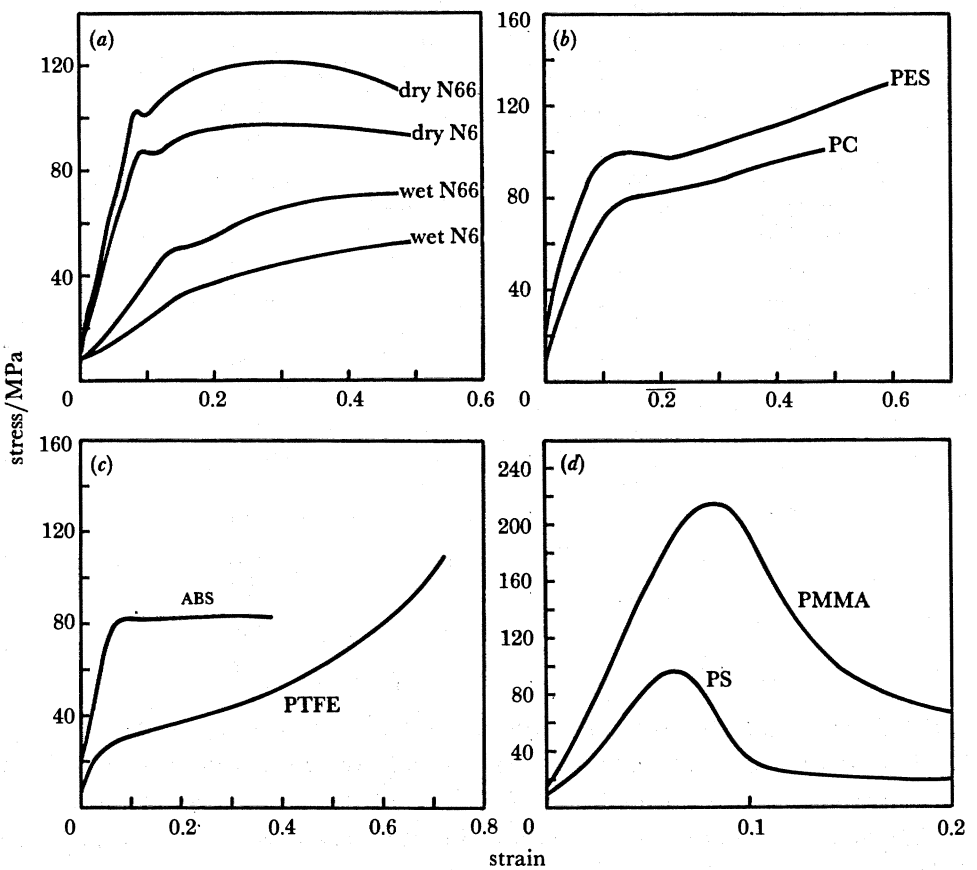

FIGURE 26. Stress–strain curves for various polymers obtained in the Kolsky bar apparatus: (*a*) wet and dry N6 and N66 ($d = 2.5$ mm, $t = 1$ mm; flat punch used); (*b*) PC ($d = 2.5$ mm, $t = 1$ mm; flat punch used) and PES ($d = 2$ mm, $t = 1$ mm; leather punch used); (*c*) ABS ($d = 2$ mm, $t = 1$ mm; leather punch used) and PTFE ($d = 2.4$ mm and 2.0 mm, $t = 0.83$ mm; flat punch used) (*d*) PMMA ($d = 2$ mm, $t = 1$ mm; flat punch used) and PS ($d = 2$ mm, $t = 0.95$ mm; flat punch used). Each curve is an average from between three and five separate experiments.

TABLE 7. SUMMARY TABLE OF FLOW STRESSES (MEGAPASCALS) OF POLYMERS AND COPPER AT THREE STRAIN RATES

material	Instron (*ca.* 10^{-2} s^{-1}) as measured	Instron (*ca.* 10^{-2} s^{-1}) corrected for friction ($\mu = m/\sqrt{3}$)	dropweight (*ca.* 10^{3} s^{-1})	Kolsky bar (*ca.* 10^{4} s^{-1})	approximate strain-rate sensitivity/MPa ($\partial\sigma/\partial \lg \dot{\epsilon}$)
dry N6	65	63	125	95	10
wet N6 (10% H_2O)	25	(*m* not measured)	49	40	5
dry N66	81	79	140	120	10
wet N66 (6.5% H_2O)	45	43	65	75	5
Noryl	$\sigma_y = 81$	77	105	90 (injection-moulded)	5
	$\sigma_t = 75$	71		110 (extrusion grade)	
PC	$\sigma_y = 70$ $\sigma_t = 61$	66 57	90	80	5
PVDF	60	57	110	$\sigma_y = 160$ (strain softens)	15
PBT	52	(m not measured)	80	$\sigma_y = 105$ $\sigma_t = 80$	5
Cu	$\sigma_y = 300$ (strain hardens)	224	$\sigma_y = 300$ (strain hardens)	$\sigma_y = 260$	—
PTFE	10 (strain hardens)	—	—	25 (strain hardens)	2.5
PMMA	—	—	—	220 (fractures)	—
PS	—	—	—	100 (fractures)	—
HDPE	—	—	—	35	—
MDPE	—	—	—	50	—
PES	—	—	100	100	—
ABS	—	—	—	82	—
CAc	—	—	—	130	—
PVC	—	—	—	125	—

as Noryl and PC, are relatively insensitive to strain rate. Furthermore, most of the polymers tested showed a *decrease* in yield stress over the decade of strain rate 10^3 to 10^4 s^{-1}. The exceptions to this were water-saturated N66, PVDF, and PBT. The form of the stress–strain curves were, in general, different at the higher strain rates. The curves obtained in the Instron invariably showed strain hardening once a critical strain characteristic of the polymer was exceeded, whereas curves obtained at the higher strain rates usually showed either flow at nearly constant stress or strain softening (see especially the Kolsky curve for PVDF). This was probably because of better lubrication and adiabatic heating. However, PTFE showed substantial strain hardening even in the Kolsky bar.

(*e*) *Synopsis of the data on the effect of strain rate*

The values of the flow or yield stresses quoted in table 7 are derived from the graphs presented in figures 13, 16, 19, 22, 23, 24 and 26. Only curves obtained under the best lubrication conditions (i.e. lowest friction) were used to compile this table. Friction corrections were only made for the low strain rate data. The values of the friction parameter m for lubricated specimens may be found in table 4 under the heading 'dynamic: from area measurement'. The friction correction for copper is large as lubrication was poor for this material. The copper specimens also had a higher value of a/h than the polymers. Perfect lubrication was assumed for the high strain rate experiments as petroleum jelly was used as lubricant, and thus the friction correction was zero in these cases. The flow stresses quoted are taken from the flat portion of the stress–strain curves wherever possible. Failing that, they are the maximum value of the 'knee' of the curve. When the curves show a yield drop, the upper yield stress is quoted as well.

The data, though admittedly limited, do not show a simple relation between yield stress and log (strain rate). In the majority of cases it would seem that some mechanism, such as adiabatic heating, gave a drop in yield stress at the highest rates of strain studied. Those that showed an increase in yield stress at these strain rates were subject to a strain rate enhancement effect suggesting some transition was being activated which more than compensated for the heat dissipated by plastic work. Rough estimates of the strain-rate sensitivity can, however, be calculated by using the low- and medium-strain-rate data, and these are given in table 7 for each polymer. The values can be seen to lie in the range 5–15 MPa per decade of strain rate for the materials investigated.

5. Conclusions and suggestions for future work

An experimental investigation has been successfully carried out into the effect of strain rate on the compressive yield stress of a wide range of polymers, taking care to identify the causes of error, and either eliminate them or measure them so that they could be corrected for. The main source of error when thin discs of material are tested in compression is friction. This was measured at both low and high rates of deformation by using photographic techniques making use of an analysis of Avitzur (1964) for the deformation of an annulus. This analysis was found to work well at a strain rate of $10^3\ s^{-1}$, but only poorly at $10^{-2}\ s^{-1}$. These techniques allowed good lubricants to be identified for the two strain-rate régimes investigated. The expression given by Gorham *et al.* (1984) for the effect of friction and specimen thickness was found to hold at low strain rates. All the polymers studied showed higher yield stresses in the high-strain-rate régime 10^3–$10^4\ s^{-1}$, but most (with the exceptions of PBT and PVDF) exhibited a softening of behaviour *within* this decade of strain rates. Their strain rate sensitivity lay between 5 and 15 MPa per decade of strain rate over the strain-rate range 10^{-2}–$10^3\ s^{-1}$. High-speed photography was invaluable for this study not only allowing measures of friction to be made during deformation, but also giving information on material failure mechanisms and associated heat evolution. Ideally in any future work, polymer specimens that are well characterized both chemically and physically should be used. It will be invaluable for the manufacturers and consumers of polymeric materials to know what effect additives, molecular mass, molecular mass distribution, microscopic structure, and crystallinity, for example, have on their rapid

deformation properties. Experiments ought to be carried out within each decade of strain rate over the range of interest to test the activated rate theory and to pick out effects due to molecular transitions, if any.

This work was funded by the Ministry of Defence (Procurement Executive). We would like to thank Dr J. Roberts and Mr R. L. Tickner of RARDE, Fort Halstead, and Dr N. S. Corney of RAE, Farnborough, for providing specimens, and for their interest and encouragement. We also thank Dr G. M. Swallowe, Dr S. N. Mentha, Dr R. Sundararajan, and Dr I. P. Hayward and Mr M. A. Parry for advice and help on various aspects of this work.

References

Adam, G. A., Cross, A. & Haward, R. N. 1975 *J. Mater. Sci.* **10**, 1582–1590.
Adams, W. W., Yang, D. & Thomas, E. L. 1986 *J. Mater. Sci.* **21**, 2239–2253.
Arridge, R. G. C. 1975 *Mechanics of polymers*. Oxford: Clarendon Press.
Ashby, M. F. & Jones, D. R. H. 1986 *Engineering Materials 2*, pp. 201–208. Oxford: Pergamon Press.
Avitzur, B. 1964 *Israel J. Technol.* **2**, 295–304.
Avitzur, B. 1968 *Metal forming: processes and analysis*, pp. 81–102. New York: McGraw-Hill.
Barham, P. J. & Arridge, R. G. C. 1979 *Polymer* **20**, 509–512.
Bauwens, J.-C. 1982 In *Plastic deformation of amorphous and semi-crystalline materials* (ed. B. Escaig & C. G'Sell), pp. 175–186. les Ulis, France: les éditions de physique.
Bauwens-Crowet, C., Ots, J. M. & Bauwens, J.-C. 1974 *J. Mater. Sci.* **9**, 1197–1201.
Booth, M. J. & Hirst, W. 1970*a* *Proc. R. Soc. Lond.* A **316**, 391–413.
Booth, M. J. & Hirst, W. 1970*b* *Proc. R. Soc. Lond.* A **316**, 415–429.
Brady, T. E. & Yeh, G. S. Y. 1971 *J. appl. Phys.* **42**, 4622–4630.
Briscoe, B. J. & Hutchings, I. M. 1976 *Polymer* **17**, 1099–1102.
Briscoe, B. J. & Nosker, R. W. 1984 *Wear* **95**, 241–262.
Briscoe, B. J. & Nosker, R. W. 1985 *Polymer Commun.* **26**, 307–308.
Briscoe, B. J. & Smith, A. C. 1981 *Polymer* **22**, 1587–1589.
Brown, N. 1971 *Mater. Sci. Engng.* **25**, 87–91.
Brown, N. & Ward, I. M. 1983 *J. Mater. Sci.* **18**, 1405–1420.
Bubeck, R. A. & Baker, H. M. 1982 *Polymer* **23**, 1680–1684.
Bucknall, C. B. & Partridge, I. K. 1983 *Polymer* **24**, 639–644.
Carr, S. H., Crist, B. & Marks, T. J. 1983 *NTIS report no.* GRI-81/0132, Washington, D.C.; National Technical Information Service.
Cheng, S Z. D. & Wunderlich, B. 1986 *J. Polymer Sci.* B **24**, 1755–1765.
Chou, S. C., Robertson, K. D. & Rainey, J. H. 1973 *Exp. Mech.* **13**, 422–432.
Clutton, E. Q. & Williams, J. G. 1981 *J. Mater. Sci.* **16**, 2583–2589.
Deopura, B. L., Sengupta, A. K. & Verma, A. 1983 *Polymer Commun.* **24**, 287–288.
Escaig, B. & G'Sell, C. (eds.) 1982 *Platic deformation of amorphous and semi-crystalline Materials*. les Ulis, France: les éditions de physique.
Evans, R. E. (ed.) 1981 *ASTM STP* 736: *Physical testing of plastics*. Philadelphia: American Society for Testing and Materials.
Field, J. E., Swallowe, G. M. & Heavens, S. N. 1982 *Proc. R. Soc. Lond.* A **382**, 231–244.
Foot, J. S., Truss, R. W., Ward, I. M. & Duckett, R. A. 1987 *J. Mater. Sci.* **22**, 1437–1442.
Fotheringham, D. G. & Cherry, B. W. 1978*a* *J. Mater. Sci.* **13**, 951–964.
Fotheringham, D. G. & Cherry, B. W. 1978*b* *J. Mater. Sci.* **13**, 231–238.
Fuller, K. N. G., Fox, P. G. & Field, J. E. 1975 *Proc. R. Soc. Lond.* A **341**, 537–557.
Gaur, U., Lau, S. F., Wunderlich, B. B. & Wunderlich, B. 1982 *J. Phys. Chem. Ref. Data* **11**, 1065–1089.
Gaur, U., Lau, S. F., Wunderlich, B. B. & Wunderlich, B. 1983*a* *J. Phys. Chem. Ref. Data* **12**, 65–89.
Gaur, U., Lau, S. F. & Wunderlich, B. 1983*b* *J. phys. Chem. Ref. Data* **12**, 91–108.
Gaur, U. & Wunderlich, B. 1980 *Macromolecules* **13**, 445–446.
Gaur, U. & Wunderlich, B. 1981 *J. Phys. Chem. Ref. Data* **10**, 119–152.
Gaur, U. & Wunderlich, B. 1982 *J. Phys. Chem. Ref. Data* **11**, 313–325.
Gaur, U., Wunderlich, B. B. & Wunderlich, B. 1983*c* *J. Phys. Chem. Ref. Data* **12**, 29–63.
Gorham, D. A. 1980 *Inst. Phys. Conf. Ser.* **47**, 16–24.
Gorham, D. A., Pope, P. H. & Cox, O. 1984 *Inst. Phys. Conf. Ser.* **70**, 151–158.
G'Sell, C. & Jonas, J.-J. 1981 *J. Mater. Sci.* **16**, 1956–1974.

Harris, J. S., Ward, I. M. & Parry, J. S. C. 1971 *J. Mater. Sci.* **6**, 110–114.
Heavens, S. N. & Field, J. E. 1974 *Proc. R. Soc. Lond.* A **338**, 77–93.
Hillig, W. B. 1985 *Polym. Engng Sci.* **25**, 339–347.
Hine, P. J., Duckett, R. A. & Ward, I. M. 1986 *J. Mater. Sci.* **21**, 2049–2058.
Hirst, W. & Lewis, M. G. 1973 *Proc. R. Soc. Lond.* A **334**, 1–18.
Hutchings, I. M. 1979 *J. Mech. Phys. Solids* **26**, 289–301.
Johnson, W. & Mellor, P. B. 1973 *Engineering plasticity*. London: van Nostrand Reinhold.
Judovits, L. H., Bopp, R. C., Gaur, U. & Wunderlich B. 1986 *J. Polym. Sci.* B **24**, 2725–2741.
Kardos, J. L., Powell, R. L. & Jerina, K. L. 1983 *NTIS report no.* GRI-81/0142. Washington, D.C.: National Technical Information Service.
Kukureka, S. N. & Hutchings, I. M. 1981 In *Proc. 7th Int. Conf. on High Energy Rate Fabrication* (ed. T. Z. Blazynski), pp. 29–38. University of Leeds.
Lataillade, J.-L., Marchand, A. & Pouyet, J. M. 1984 In *Proc. 9th Int. Congress on Rheology: Advances in Rheology vol. 3: Polymers* (ed. B. Mena, A. Garcia-Rejon, C. Rangel-Nafaile), pp. 137–146. National Autonomous University of Mexico.
Lataillade, J.-L., Pouyet, J. M., Hamdy, A. & Signoret, C. 1980 *Journée de Mécanique Physique*, Université de Bordeaux I.
Lau, S. F., Suzuki, H. & Wunderlich, B. 1984*a* *J. Polym. Sci.* B **22**, 379–405.
Lau, S. F., Wesson, J. P. & Wunderlich, B. 1984*b* *Macromolecules* **17**, 1102–1104.
Lefebvre, J. M., Escaig, B., Coulon, G. & Picot, C. 1985 *Polymer* **26**, 1807–1813.
Male, A. T. & Depierre, V. 1970 *Trans. Am. Soc. mech. Engrs.* F **92**, 389–397.
Mascia, L. 1974 *The role of additives in Plastics*. London: Edward Arnold.
Michler, G. H. 1986 *Polymer* **27**, 323–328.
Olley, R. H., Hodge, A. M. & Bassett, D. C. 1979 *J. Polym. Sci.* B **17**, 627–643.
Pampillo, C. A. & Davis, L. A. 1971 *J. appl. Phys.* **42**, 4674–4679.
Pope, P. H. 1986 PhD Thesis, University of Cambridge.
Pope, P. H. & Field, J. E. 1984 *J. Phys.* E **17**, 817–820.
Starkweather, H. W. Jr., Zoller, P. & Jones, G. A. 1984 *J. Polym. Sci.* B **22**, 1615–1621.
Steer, P. 1986 Thèse de Docteur en Science des Matériaux, no. 16, Univ. des Sciences et Techniques de Lille Flanders Artois.
Steer, P., Rietsch, F., Lataillade, J.-L., Marchand, A. & El Bounia, N.-E. 1985 *J. Phys. (Paris) Colloq.* **46** (C5), 415–423.
Struik, L. C. E. 1978 *Physical ageing in amorphous polymers and other materials*. Amsterdam: Elsevier.
Swallowe, G. M. & Field, J. E. 1982 *Proc. R. Soc. Lond.* A **379**, 389–408.
Swallowe, G. M., Field, J. E. & Horn, L. A. 1986 *J. Mater. Sci.* **21**, 4089–4096.
Taylor, G. I. 1938 *J. Inst. Metals* **62**, 307–324.
Timoshenko, S. P., Goodier, J. N. 1970 *Theory of elasticity*, 3rd edn, p. 408. Tokyo: McGraw-Hill Kogakusha.
Truss, R. W., Clarke, P. L., Duckett, R. A. & Ward, I. M. 1984 *J. Polym. Sci.* B **22**, 191–209.
Truss, R. W., Duckett, R. A. & Ward, I. M. 1981 *J. Mater. Sci.* **16**, 1689–1699.
Turner, S. 1983 *Mechanical testing of plastics*, 2nd edn. New York: Longman.
Vinh, T. & Khalil, T. 1984 *Inst. Phys. Conf. Ser.* **70**, 39–46.
Walley, S. M. & Field, J. E. 1987 *Phil. Trans. R. Soc.* A **321**, 227–303.
Walley, S. M., Field, J. E. & Greengrass, M. 1987 *Wear*, **114**, 59–71.
Walley, S. M., Field, J. E., Swallowe, G. M. & Mentha, S. N. 1985 *J. Phys. (Paris) Colloq.* **46** (C5), 607–616.
Ward, I. M. 1984 *Polym. Engng Sci.* **24**, 724–736.
Whitney, W. & Andrews, R. D. 1967 *J. Polym Sci.* C **16**, 2981–2990.
Wiesbuch, K. & Richter, R. 1986 *J. Mater. Sci.* **21**, 3302–3316.
Williams, J. G. & Hodgkinson, J. M. 1981 *Proc. R. Soc. Lond.* A **375**, 231–248.
Wingert, L. E. 1962 U.S. Patent no. 3031329.
Wright, D. G. M., Dunk, R., Bouvart, D. & Autran, M. 1988 *Polymer* **29**, 793–796.

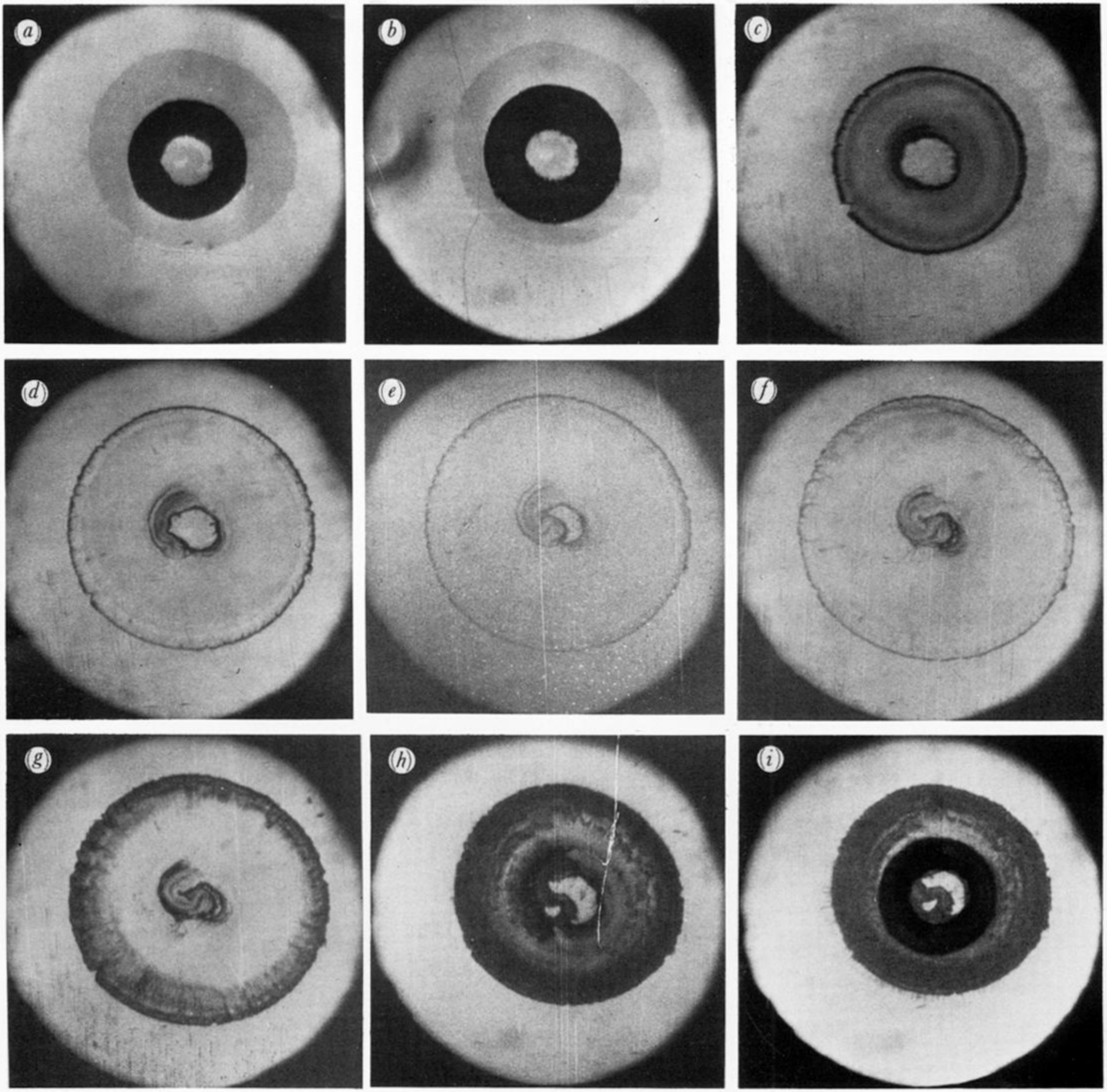

FIGURE 2. High-speed photographic sequence of the unlubricated deformation of a commercial nylon washer (initial dimensions: OD = 6.3 mm, ID = 3.1 mm, thickness = 0.8 mm. Times in microseconds from moment of impact: (*a*) 0; (*b*) 70; (*c*) 140; (*d*) 210; (*e*) 280; (*f*) 420; (*g*) 560; (*h*) 630; (*i*) 700. Note the asymmetric closing of the hole after *ca.* 210 μs and the overwriting in frame (*i*) allowing direct comparison between initial and final states and revealing near perfect uniaxial loading. Unloading is taking place in frames (*g*)–(*i*).

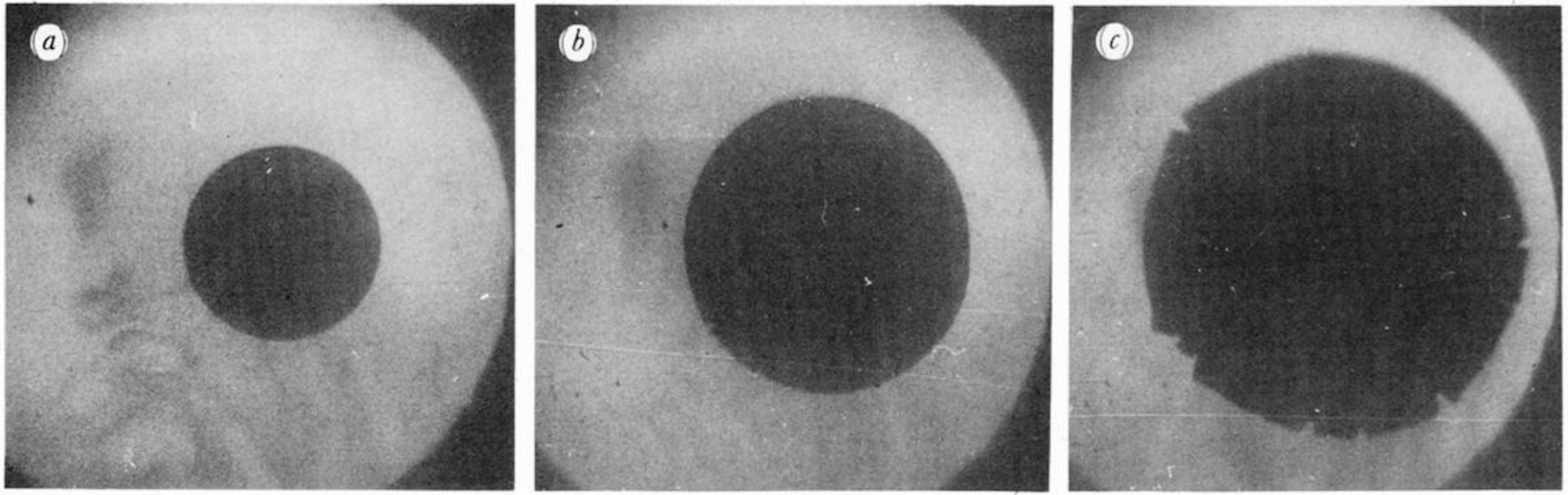

FIGURE 3. High-speed photographic sequence of the deformation and failure of a 1 mm thick and 5 mm diameter Noryl disc (extrusion grade). Times in microseconds from moment of impact (*a*) 0; (*b*) 195; (*c*) 236.

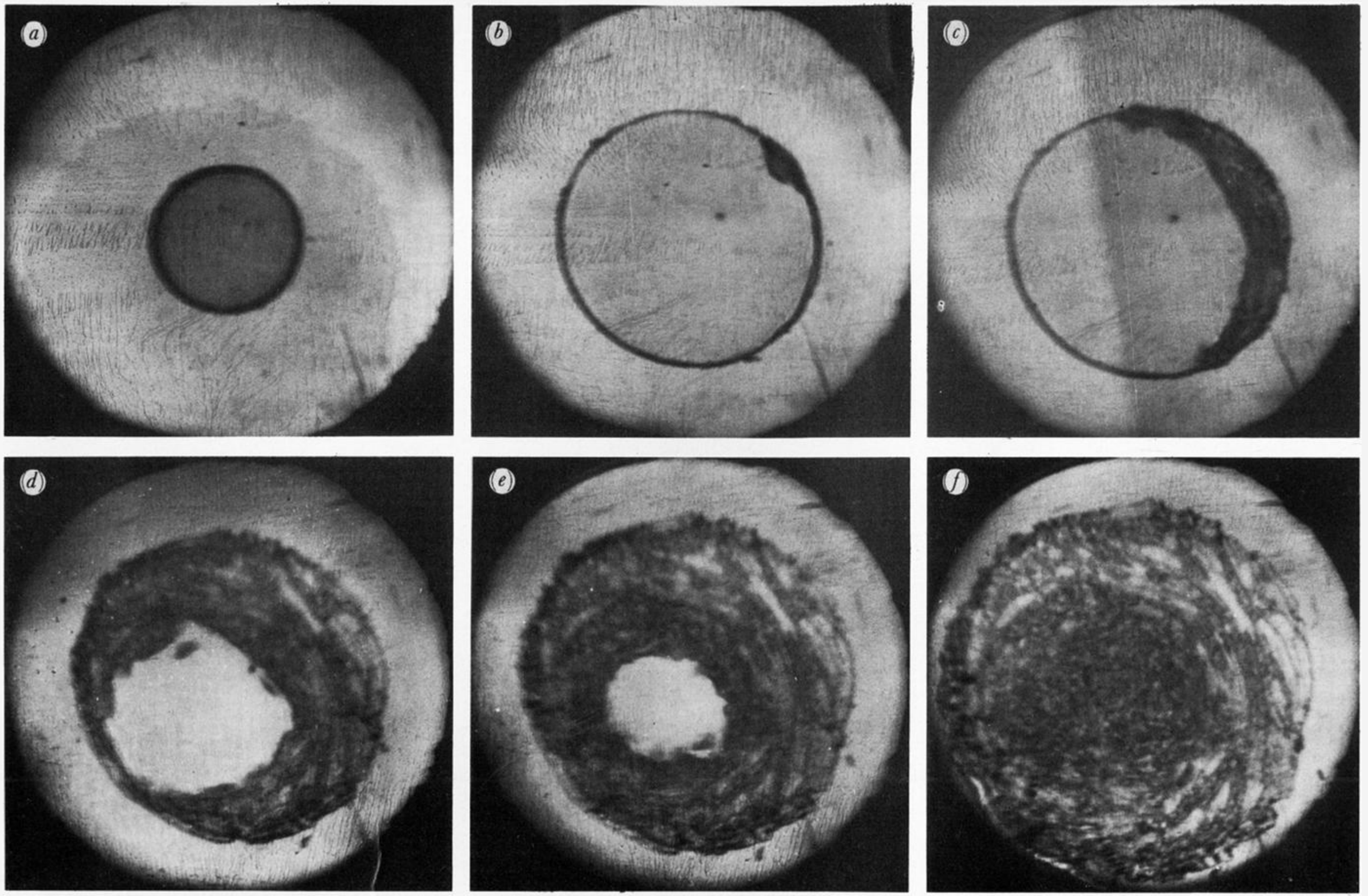

FIGURE 4. High-speed photographic sequence of the deformation and failure of a 1 mm thick and 6.5 mm diameter disc of PES. Times in microseconds from moment of impact: (*a*) 0; (*b*) 263; (*c*) 284; (*d*) 305; (*e*) 312; (*f*) 327.

(*a*)

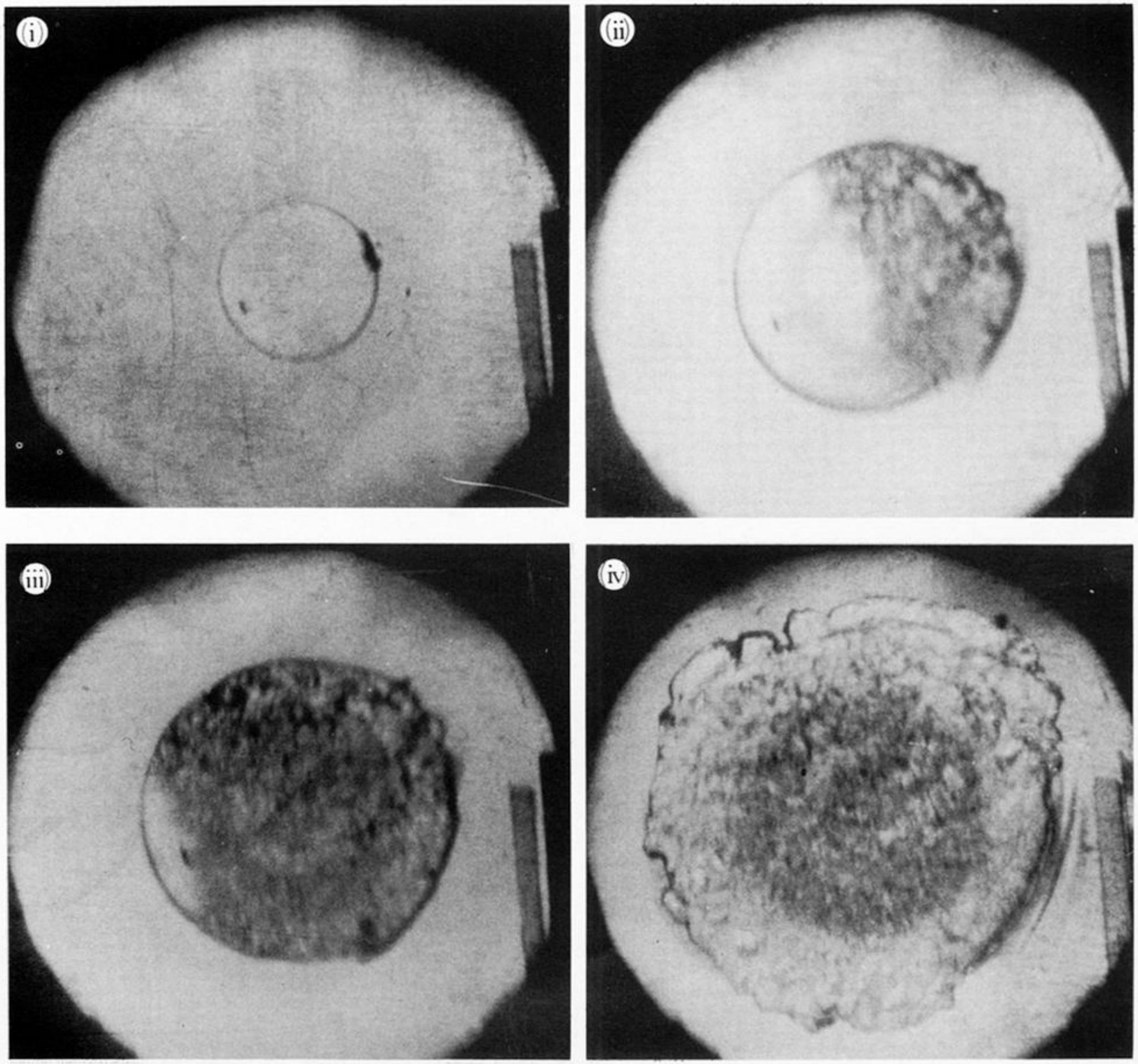

FIGURE 6*a*. High-speed photographic sequence of the deformation of a 1 mm thick and 5 mm diameter disc of PC in contact with heat-sensitive film. Note the development of a ring of discolouration roughly commensurate with the original diameter of the disc, and the buckling of the heat-sensitive film in frame (iv). The darkening of the film during fracture is clearly visible. Times in microseconds from moment of fracture: (i) initial disc; (ii) 7; (iii) 14; (iv) 126. (The original was in colour.)

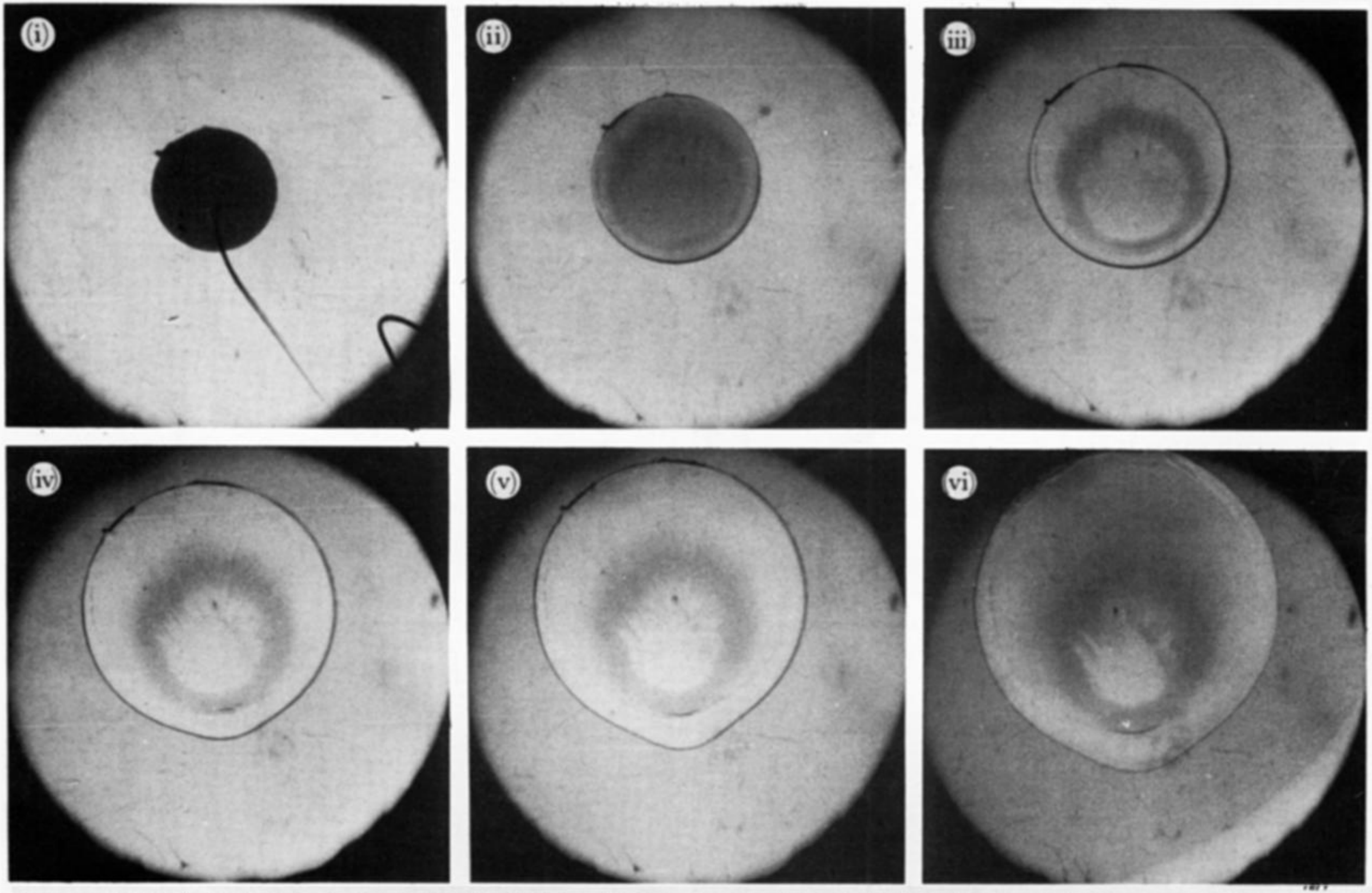

FIGURE 6*b*. Deformation of a 1 mm thick and 5 mm diameter, dry N6 disc in contact with heat-sensitive film. Times in microseconds from moment of impact: (i) 0, (ii) 133; (iii) 175; (iv) 210; (v) 224; (vi) 350. The darkening of the film is clearly visible as a ring that spreads inwards and outwards. The lines in frame (i) were caused by dirt on the camera mirror.

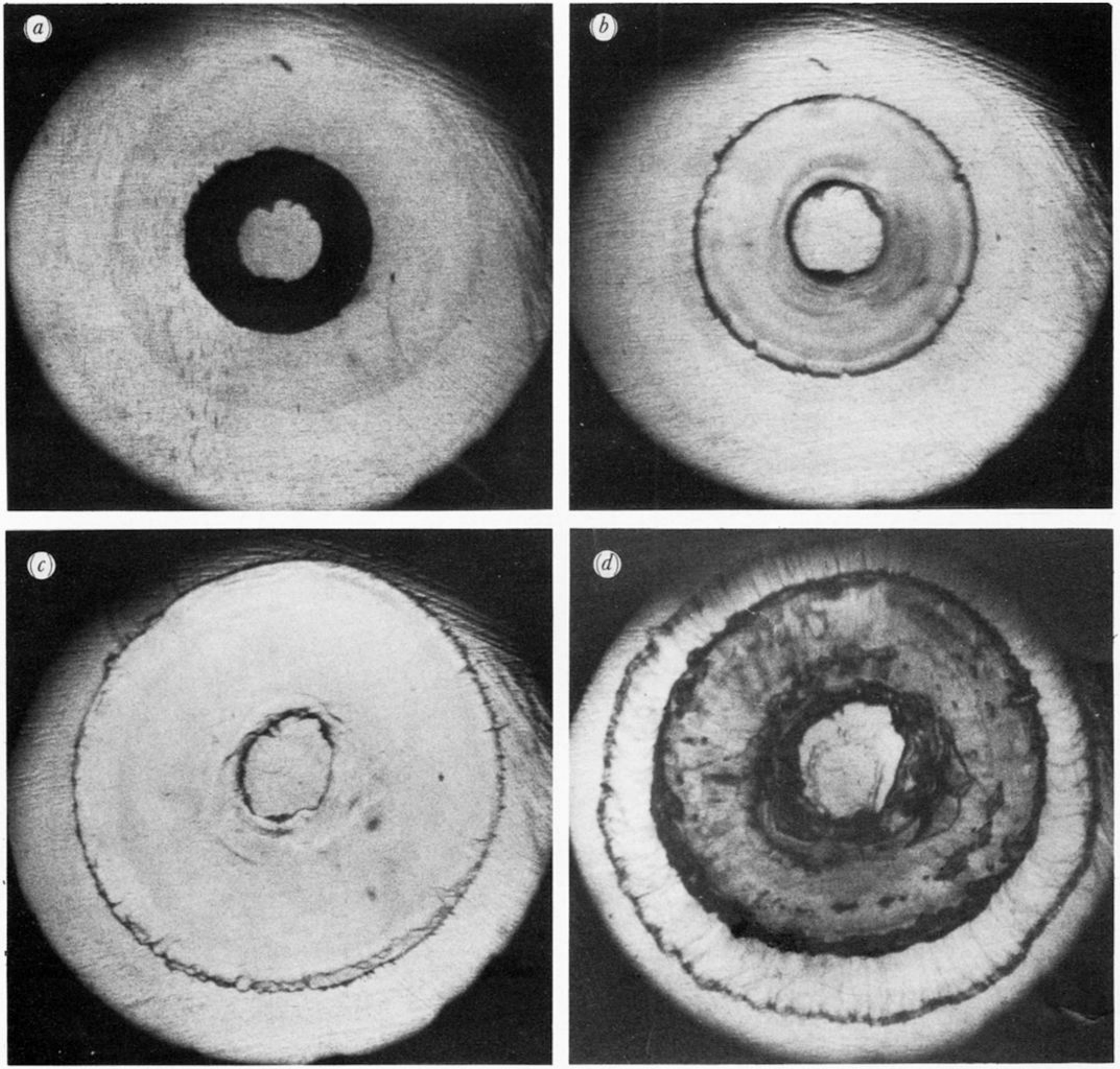

FIGURE 8. High-speed photographic sequence of the deformation of a commercial nylon washer (dimensions given in figure 2) lubricated by gun barrel oil. Times in microseconds from the moment of impact: (*a*) 0; (*b*) 140; (*c*) 210; (*d*) 630. Note in frame (*d*) the substantial relaxation that has occurred on unloading.

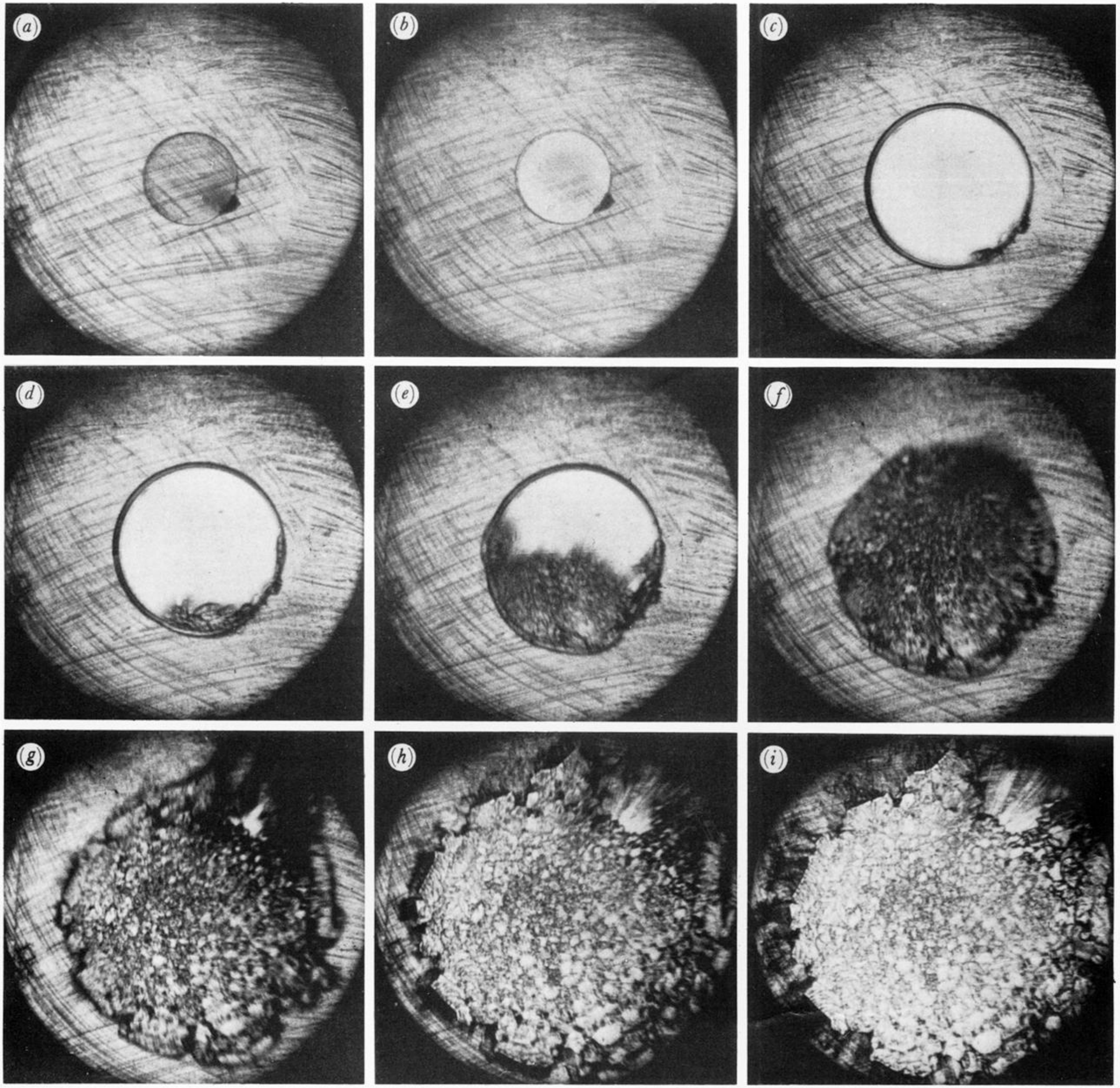

FIGURE 11. High-speed photographic sequence of a 1 mm thick and 5 mm diameter PC disc deforming in the presence of petroleum jelly lubricant. Times in microseconds from the moment of impact: (*a*) 0; (*b*) 14; (*c*) 234; (*d*) 241; (*e*) 248; (*f*) 255; (*g*) 262; (*h*) 269; (*i*) 276.

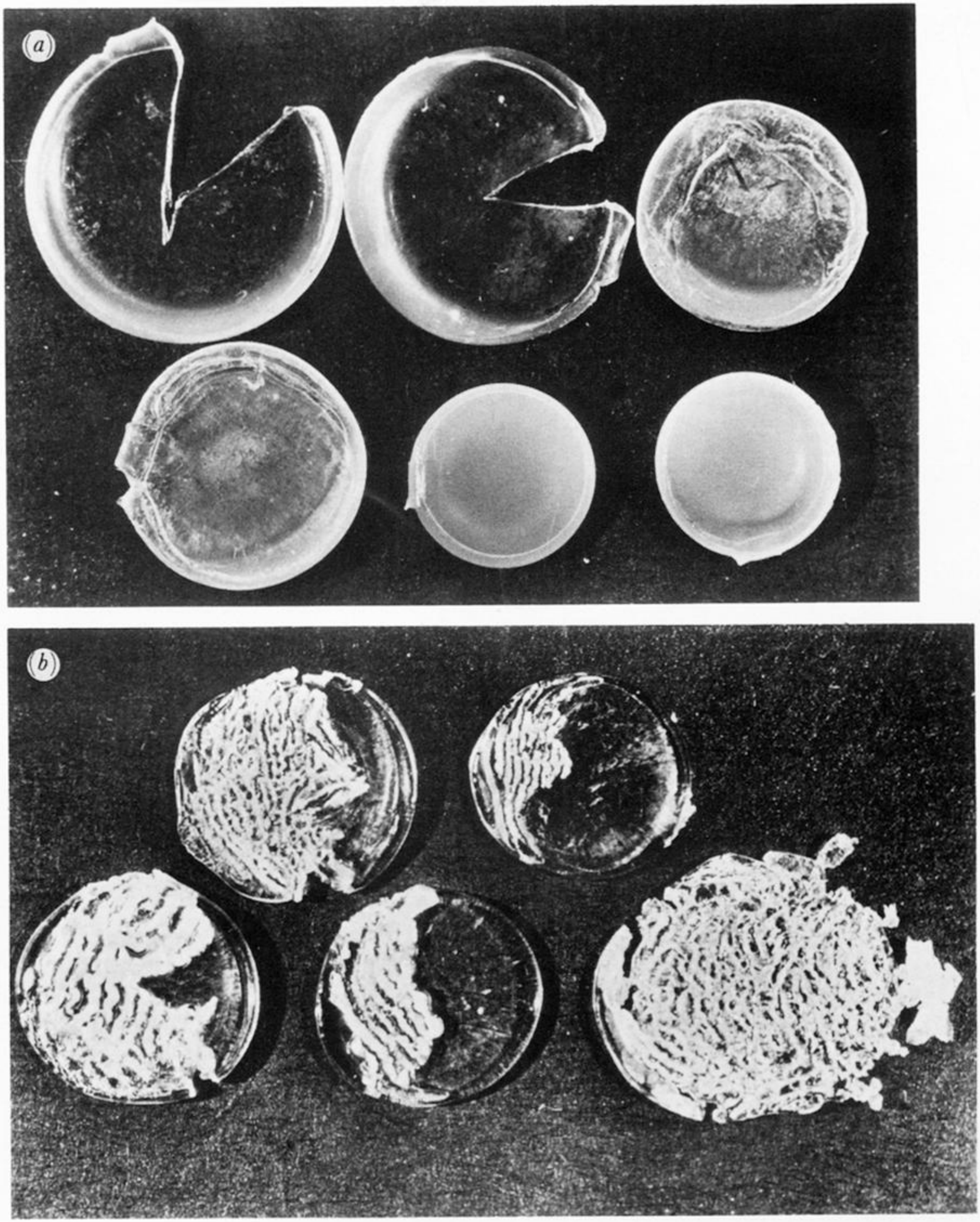

FIGURE 20. Specimens after deformation in the dropweight apparatus: (*a*) 2 mm thick dry N6; (*b*) 1 mm thick PC. Failure was by shear banding.

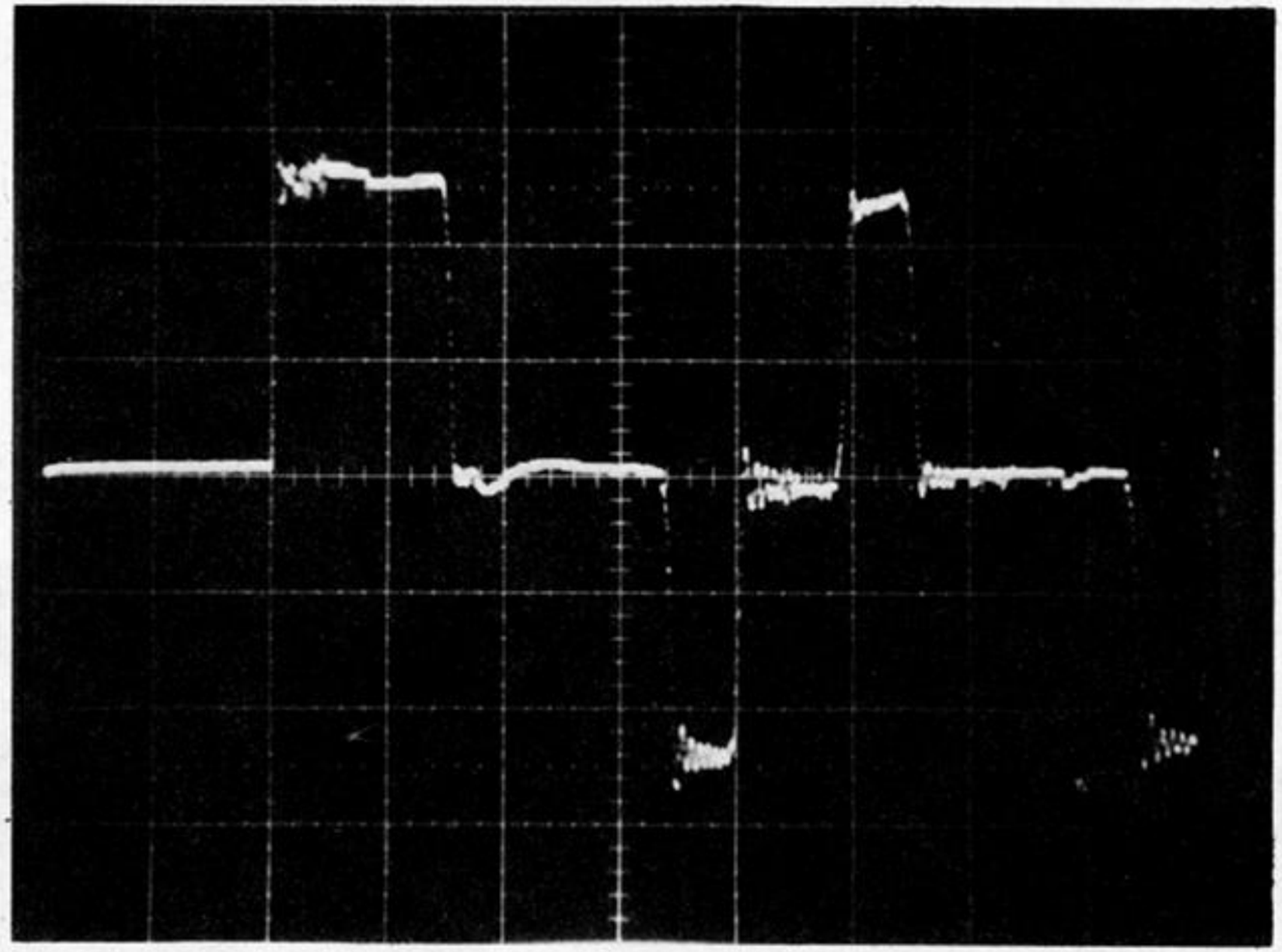

FIGURE 21. Strain gauge output from direct impact of 75 mm long silver steel rod 3 mm in diameter on WC output bar, 213 ± 2 mm long and 3.17 mm in diameter. The length of the initial compressive pulse gives the impedance of the striker. The time from the beginning of the compressive pulse to the return of the first tensile pulse gives the impedance of the output bar (see table 6).